DOI: 10.1002/anie.200805503

Ultracold Chemistry

Cold Molecules: Preparation, Applications, and Challenges

Melanie Schnell and Gerard Meijer*

Keywords:
cold molecules ·
high-resolution spectroscopy ·
molecular beams ·
Stark deceleration ·
ultracold chemistry

Research with cold molecules has developed rapidly in recent years. There is now a variety of established methods for cooling molecules into the millikelvin range. Nevertheless, a focal point of current research is directed toward finding new ways to bring the temperature of molecules even closer to absolute zero. Samples of cold molecules offer not only important applications for high-resolution spectroscopy, which benefit from the increased interaction time of slow molecules with electromagnetic radiation; they also promise access to an exotic regime of chemical reactivity, in which phenomena such as quantum tunneling and quantum resonances predominate. This review begins with an introduction to the methods by which cold molecules can be prepared, with special emphasis on Stark deceleration and traps. In addition to applications of cold molecules that have already been partially achieved, an important focus of the review concentrates on possible future applications, and both aspects are illustrated with selected examples.

From the Contents

1. Introduction

In the past two decades, physicists have learned how to cool atoms to ever lower temperatures and to gain increasing control over them during these processes. Successful cooling of atoms to the point of quantum degeneracy has revolutionized atomic physics and quantum optics. One of the high points was certainly the achievement of Bose–Einstein condensates of atoms, which were predicted theoretically as early as 1924 by Satyendranath Bose and Albert Einstein,[1] but not experimentally demonstrated until 71 years later, in 1995.[2–4] Other very interesting applications include atom interferometry, extremely precise laser spectroscopy,[5] and atom lasers.[3,4]

In view of the fascinating and rapid developments in the field of ultracold atoms, it comes as no surprise that experimentalists would like to play the same games with molecules. Molecules are fundamentally different from atoms; some would say more interesting, but certainly more complicated. A molecule consists of a structured configuration of atoms that can be subjected to dynamic changes, such as the transition between different conformers. Because of their complex spatial structure, molecules, in contrast to atoms, also possess both rotational and vibrational degrees of freedom. This broad diversity of rotational and vibrational quantum states introduces new dimensions into possible experiments. Moreover, molecules have properties not present in atoms, such as permanent electric dipole moments. Precisely these differences between atoms and molecules are of fundamental significance for many physicochemical processes in general and for the preparation of cold species in particular. Atoms are usually cooled by so-called laser cooling, in which the photons of a laser beam transfer their momenta to atoms, thereby reducing their velocity.[6] This requires multiple passes through the same absorption–emission cycle, which is achieved by so-called closed-cycle transitions for many atoms. Such closed-cycle transitions are extremely rare for molecules owing to their complex vibrational and rotational energy level structure, which furthermore are even coupled. Consequently, an efficient momentum transfer is impossible, and laser cooling of molecules is inapplicable in the vast majority of cases. For this reason it has been necessary to develop other methods for the cooling of molecules that are presented and elaborated in this Review. At the same time, it is precisely these differences between atoms and molecules that make research on cold molecules so interesting: cold polar molecules undergo strong dipole–dipole interactions, which can be exploited for quantum computing with polar molecules.

First, the question arises: what precisely is meant by cold atoms and molecules? According to Maxwell, the temperature of a gas characterizes the velocity distribution of the atoms or molecules in that gas. In other words, a narrow velocity distribution of the molecules in a sample is associated with a low temperature. A velocity distribution with a half-width of 5 $m\,s^{-1}$ for ammonia molecules corresponds roughly to a temperature of only 30 mK. Therefore, cold molecules are slow molecules. A distinction is often made between cold ($1\,K > T > 1\,mK$) and ultracold ($T < 1\,mK$) species. Under most of the experimental conditions described below, the system under investigation is not in thermodynamic equilibrium, so strictly speaking, no temperature can be ascribed to it. Nevertheless, the temperature T is utilized as a way of expressing the kinetic energy of the molecules, which is linked with the temperature through $E_{kin} \approx k_B T$ (k_B: Boltzmann constant). Moreover, as indicated, molecules have various internal degrees of freedom: of electronic nature, vibrational, rotational, and nuclear spin. It is often advantageous (see also Section 6) if the cold molecules are in a particular quantum

[*] Dr. M. Schnell, Prof. Dr. G. Meijer
Fritz-Haber-Institut der Max-Planck-Gesellschaft,
Faradayweg 4–6, 14195 Berlin (Germany)
Fax: (+49) 30-8413-5603
E-mail: schnell@fhi-berlin.mpg.de

state; for example, in the absolute rovibronic (i.e., the rotational, vibrational, and electronic) ground state.

The possible applications of cold molecules are manifold, of practical as well as elementary nature, stretching thematically over many areas of physics and chemistry. A current and very comprehensive overview of cold molecules is provided in the book *Low Temperatures and Cold Molecules*.[7] First, it is advantageous, if not absolutely necessary, for many experiments to have as complete control as possible over all degrees of freedom of the molecules. This includes not only the degrees of freedom of the center of gravity motion, but also internal degrees of freedom. Moreover, cold molecules are ideally suited for high-resolution spectroscopy[8,9] and precision measurements. Experiments of this sort promise revolutionary findings, such as an experimental determination of the extremely small energy differences between enantiomers of chiral molecules.[10–13] These small energy differences result from the parity-violating nature of the weak interaction. It is also anticipated that cold polar molecules will play a key role in experiments designed to determine the permanent electric dipole moment of electrons,[14] or a possible variation of fundamental constants of nature with time.[15–18] The long interaction time of trapped cold molecules with electromagnetic radiation can be used to measure directly the lifetime of a long-lived electronic or vibrational quantum state.[19–21] With other molecular beam methods, this has so far been possible only indirectly, and thus relatively imprecisely.

Another exciting route is the study of (ultra)cold chemistry. Cold molecules promise entry into an exotic realm of chemical reactivity in which phenomena such as quantum tunneling and quantum resonance prevail.[22–25] At these low kinetic energies, interesting effects have been predicted for molecular collisions. In general, a distinction is made between elastic, inelastic, and reactive collisions. In an elastic collision, the colliding partners may exchange kinetic energy, while the overall kinetic energy of the system remains intact. In an inelastic collision, on the other hand, a portion of the kinetic energy is transformed into internal energy, which is to say that at least one of the reacting partners changes quantum states. In the ultracold regime, the effective cross-sections for elastic and inelastic collisions show sharp resonances, as the (very low) collision energies are of the same order of magnitude as rotational energies in the collision complex.[23,26,27] After a collision, the reduced translational energy of the molecules is no longer sufficient to overcome their mutual Van der Waals attractions, so that the molecules are temporarily bound to each other.

This Review begins with an introduction to the techniques of creating cold molecules, with an emphasis on molecular beam methods in general and Stark deceleration in particular, which has become an established procedure in research on cold polar molecules in the course of the last decade. Special attention is directed toward molecular traps, which make it possible to store cold molecules for several seconds and thereby study molecular properties and their interactions in detail. An additional section deals with applications of cold molecules: both those that have already been realized, and those that are conceivable in the future.

2. Preparation of Cold Molecules

Laser cooling followed by evaporative cooling are the decisive techniques for preparing cold atoms. Evaporative cooling should also be applicable to molecules, provided that their elastic and inelastic collision cross-sections at low temperatures are similar to those of atoms; however, this has yet to be demonstrated experimentally. As indicated, laser cooling of molecules is difficult, because the required closed transitions are not available owing to the complex energy-level structures in molecules.

Several alternatives for preparing cold molecules have therefore been developed in recent years (Table 1). Some methods proceed from laser-cooled atoms, which are combined to give dimers, whereas others begin directly with the molecules to be studied, which are then cooled. In this way larger and more complex molecules can also be treated.

For the preparation of cold molecules from a very dense ensemble of laser-cooled atoms, energy and momentum conservation require interaction with a third body. If this third body is a photon, molecule formation occurs through photoassociation. If another collision partner is available, molecule formation can take place as well. In a third approach, the change of a magnetic field can be used to convert the two atoms into a bound state by passage through a Feshbach resonance. The photoassociation method and exploitation of Feshbach resonances are both very successful and widespread, especially in the field of atomic physics, and

Melanie Schnell, born in 1978, studied chemistry at the Universities of Hannover and Bonn. She earned her doctorate in 2004 under Jens-Uwe Grabow in Hannover on rotational spectroscopic and group theoretical studies of intramolecular interactions of flexible molecules. After a research stay with Jon T. Hougen at NIST in Gaithersburg, she joined the department of Gerard Meijer at the Fritz Haber Institute in 2005. There she became involved in developing traps for polar molecules and in the manipulation of cold molecules using microwave radiation. Since 2005 she has been supported by a Liebig Fellowship of the Fonds der Chemischen Industrie.

Gerard Meijer, born in 1962, is a pioneer of the Stark deceleration technique. In 1995 he became a professor in Nijmegen, and in 2000 Director of the FOM Rijnhuizen Institute for Plasma Physics in Nieuwegein, Netherlands. There he initiated the research program on cold molecules, and using the free-electron laser FELIX carried out IR-spectroscopic experiments on molecules in the gas phase. Since 2003 he has been director of the Department of Molecular Physics at the Fritz Haber Institute of the Max Planck Society.

Table 1:
Methods employed to date for producing (ultra)cold molecules, the temperatures T reached for trapped samples or final velocities v for decelerated samples that were not trapped, and the number N of molecules in the sample.

Method	Molecule	T or v	N
photoassociation	Rb_2, Cs_2, He_2^*, H_2, Li_2, Na_2, K_2, Ca_2, KRb, RbCs, NaCs, LiCs, LiRb	30 μK	2×10^5
Feshbach resonances	Li_2, K_2, Cs_2, Rb_2, Na_2, Cs_3, KRb	50 nK	$>10^5$
buffer-gas cooling	CaH, CaF, VO, PbO, NH, ND, CrH, MnH	400 mK	$>10^8$
velocity filters	H_2CO, ND_3, S_2, D_2O	1 K	10^9 molecules/s
Stark deceleration and trapping	$^{14}NH_3$, $^{15}NH_3$, $^{14}ND_3$, $^{15}ND_3$, CO*, OH, OD, NH*, SO_2, YbF, H_2CO, C_7H_5N	5 mK	10^6
Rydberg deceleration	H_2	-10% E_{kin}	no data
Zeeman deceleration	O_2	50 m s^{-1}	no data
optical deceleration	C_6H_6, NO	295 or 242 m s^{-1}	no data
collision/reactions	NO/KBr	400 mK/15 m s^{-1}	no data
mechanical methods	O_2, CH_3F, perfluorinated C_{60}	70 or 11 m s^{-1}	no data

they will therefore be described briefly in what follows. For a detailed description the reader is directed to the review articles in reference [28–33].

The principle of photoassociation was suggested[34] as early as 1987, and experimentally demonstrated for the first time in 1993 using Na_2 and Rb_2.[35,36] Many experimental and theoretical papers have subsequently appeared related to photoassociation of ultracold atoms, and these have been summarized for example in a review article by Jones et al.[31] Two colliding atoms jointly absorb a photon, through which they may be transformed into a dimer in a particular excited state (Figure 1, process 1). The resulting molecules are however short-lived, and they largely decay through spontaneous emission into the atoms (process 2). To obtain stable molecules, they must be transferred from a specific rovibronic level v′ of the electronically excited state into a bound level v of the electronic ground state or a low-lying triplet state (process 3). This stabilization process involves either spontaneous emission or induced emission with a second laser.

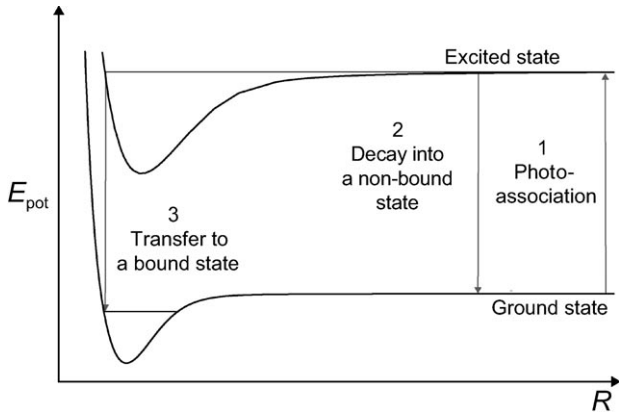

Figure 1. Principle of photoassociation (E_{pot} = potential energy, R = internuclear distance). Two ultracold atoms colliding with one another collectively absorb a photon, whereby they can be excited to a specific electronically excited state of the dimer (process 1). To avoid a decay back into the non-bound state (process 2), the molecules must be transferred to a bound level v of the electronic ground state or a low-lying triplet state (process 3), which occurs through either spontaneous or induced emission.

In addition to generating very cold samples of dimers, photoassociation has developed into an important tool for molecular spectroscopy in the last two decades, in that it provides information on the long-range part of molecular potential curves as well as on other collision parameters of atoms at very low energies, such as the scattering length and positions of Feshbach resonances.[31]

The second approach to preparing ultracold molecules in an indirect way from ultracold atoms involves the Feshbach resonances mentioned above.[32,33,37–39] In the ultracold regime, the collision of two atoms is described with the aid of the scattering length, which is very sensitive to changes in the molecular interaction potential. If the atoms, the resulting molecule, or both are paramagnetic, this interaction potential can be altered with an external magnetic field (Figure 2a).[37] Under specific conditions, it thus becomes possible that the energies of the non-bound state (the pair of atoms) and the bound state (the dimer) become identical. This condition is referred to as Feshbach resonance. When the magnetic field is made to pass through a Feshbach resonance, a non-bound pair of atoms can be transformed into the bound molecular state. Dimer formation takes place on that side of the Feshbach resonance which is associated with a positive scattering length ($a>0$) (Figures 2a and b). The binding energy of the molecule is very low, only a few mK. Nevertheless, this method has been successfully applied to prepare dimers and even trimers[40] (Table 1).

One advantage of photoassociation and Feshbach resonances is that the resulting dimers have the same low translational temperature as the laser-cooled starting atoms; that is, they are ultracold. Moreover, molecular samples prepared in this way exhibit a high phase-space density. The phase-space density is dependent upon the density of the molecular cloud and upon the thermal De Broglie wavelength Λ: $\rho=\Lambda^3 n$. Λ is defined as $\Lambda=h/(2\pi m k_B T)^{1/2}$, where h is Planck's constant, m is the mass of the particle, k_B is Boltzmann's constant, and T is the temperature of the gas. A high phase-space density, required for the formation of Bose–Einstein condensates, can thus be achieved with very low temperatures and/or very high densities. Both apply to molecular assemblies prepared by photoassociation or at Feshbach resonances. Typically, temperatures in the nanokelvin range and densities of $n\approx10^{13}$–10^{15} atoms per cubic

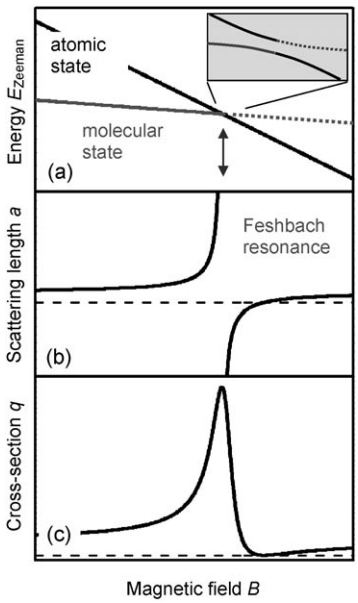

Figure 2. A Feshbach resonance can arise through coupling between an atomic scattering state and a bound molecular state. In the process, the non-bound atom pair is transferred to the bound molecular state. a) The Zeeman energy E_{Zeeman} of the states as a function of an external magnetic field B. At a particular magnetic field (indicated by the arrow), the states cross. Coupling of the states leads to an "avoided crossing" (see inset). The s-wave scattering length a diverges at this point (b), and the elastic cross-section q (c) shows a strong resonant behavior (reproduced with permission from Ref. [37]).

centimeter are attained. The first Bose–Einstein condensate (BEC) of molecular dimers was prepared from laser-cooled atoms in 2003.[41–43]

As indicated, dimer formation and thus the formation of a BEC of dimers occur on the side of a Feshbach resonance that is associated with a large, positive scattering length a ($a > 0$). Dimers can also be formed on the other side of the resonance ($a < 0$): the ground state of the resulting system near 0 K is a Fermionic superfluid, and can be understood in the context of the Bardeen–Cooper–Schrieffer (BCS) theory. The two extremes, BEC and BCS, are connected through a transition region in which the gas is subject to strong interactions.[33,44] In recent years, many spectacular results have been achieved with the condensation of molecules in the BEC-BCS transition region, and they have been described for example in the review in Ref. [33].

Disadvantageous for chemical applications is the fact that to date, the methods have been limited to the formation of alkali metal dimers and one trimer (Table 1). An additional disadvantage is that the molecules prepared in that way often occur in rotationally and vibrationally excited states, which are unstable with respect to collisions; that is, they still possess a large amount of internal energy. Therefore, a primary goal of current experimental efforts is the development of efficient techniques that permit the transfer of excited and only weakly bound molecules to their lowest rotational and vibrational (rovibrational) state without major losses.[45] This was recently achieved simultaneously by several groups. One group generated LiCs molecules by photoassociation with the absorbed photons chosen such that the resulting molecules were not excited. Instead, 23% were converted into the ground state through spontaneous emission.[46] In a further experiment, photoassociated Cs_2 was transferred with a broadband femtosecond laser through vibrational redistribution to the vibrational ground state $v = 0$ of the electronic ground state.[47] In another approach, KRb molecules[48] and Rb_2 and Cs_2 molecules[49,51] were prepared using the Feshbach resonance method as a first step. To transform the loosely bound "Feshbach molecules" into tightly bound molecules in their rovibrational ground states, both groups used the STIRAP (stimulated Raman adiabatic passage) procedure.[50] In this method, a molecule is subjected to two laser beams of differing frequency that couple the initial and final states of the molecule with an electronically excited molecular state (Figure 3). In other words, the STIRAP procedure is an

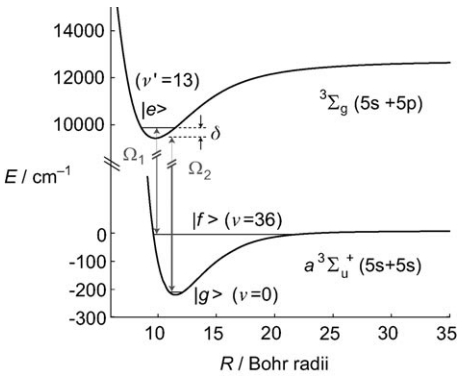

Figure 3. Potential energy curves and energy levels for the molecule Rb_2. The internuclear distance R is given in Bohr radii. Lasers 1 and 2 couple the energy levels $|f>$ and $|g>$ with the excited level $|e>$ with Rabi frequencies $\Omega_{1,2}$. The STIRAP method [50] allows the population of the state $|f>$ to be transferred to the state $|g>$ (reproduced with permission from Ref. [49]).

optical method that enables the population of the state $|f>$ to be transferred into the state $|g>$. In this way, up to 87% of the Rb_2 molecules could be transferred into the lowest rovibrational state of the triplet potential $a^3\Sigma_u^+$.[49] Furthermore, it was possible to prepare KRb molecules in their singlet rovibrational ground state with 83% efficiency.[48]

Apart from these associative, indirect methods for preparing ultracold dimers from ultracold atoms, there is a variety of methods that directly cool the desired molecules. One approach to preparing molecules at low temperatures makes use of superfluid helium droplets. Molecules embedded in the droplets adopt the low temperatures of their cold helium environment ($T \approx 0.4$ K). Helium droplets have found wide application in molecular spectroscopy in particular, but also for the preparation and investigation of highly reactive, transient species, such as radicals.[52] As this Review mainly concentrates on isolated, neutral cold molecules, the interested reader is referred to recent review articles.[52–55] Similarly, an appropriate treatment of results in the field of cold ions, which are especially important for (interstellar)

chemistry and spectroscopy, exceeds the scope of this article. For a current overview of this broad topic, it is recommended that the reader consult the corresponding book chapters in reference [56,57].

Buffer-gas cooling is, in principle, a general method. It can be applied to the direct cooling of both molecules and atoms, as it depends only on their elastic scattering cross-sections. The particles are introduced into a buffer-gas cell, where they collide with cold helium and thermalize, thereby adopting the temperature of the helium gas (550 mK for ^{3}He; Figure 4). In addition, a pair of superconducting coils in anti-Helmholtz configuration surrounds the buffer-gas cell and thereby form a spherical, magnetic quadrupole field in which buffer-gas-cooled paramagnetic species can be trapped. In this way it was possible to first cool and then trap molecules such as CaH,[58] PbO,[59] CrH, and MnH,[60] as well as NH radicals.[21] With this method, it is possible to prepare large amounts of cold molecules ($N > 10^8$ molecules; see Table 1).

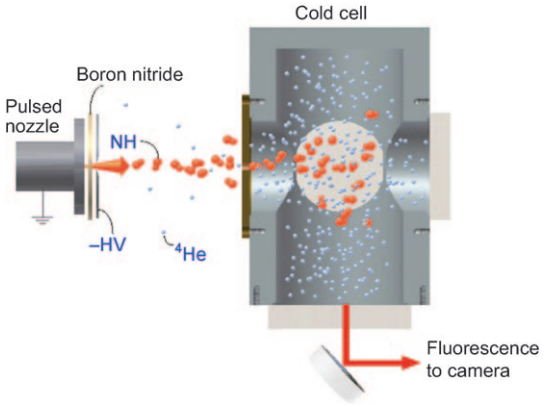

Figure 4. The principle of buffer-gas cooling. A molecular beam of NH radicals is let into a buffer-gas cell, where the NH molecules thermalize with the helium buffer gas and are stored in a magnetic quadrupole trap. The buffer gas is subsequently pumped out. HV = high voltage. (Reproduced from http://www.doylegroup.harvard.edu/molecule/molecule.html.)

Apart from its versatility, this method is also of interest because it can be used to generate beams of cold molecules.[59,61] Through a small hole, buffer-gas-cooled molecules escape effusively from the buffer-gas cell. These cold molecular beams are then available for various applications.

Other methods take advantage of the fact that in every thermal gas, slow (and therefore cold) molecules are present, according to the Maxwell velocity distribution. These molecules can be filtered out. Starting with an effusive molecular beam of, for example, formaldehyde, and taking advantage of the Stark effect, the slow fraction of molecules from the velocity distribution can be selected with the aid of a curved electric filter or guide.[62] Only the slow molecules will follow the curve of the filter, whereas the faster ones fly on almost undisturbed. In this way, molecules are obtained with longitudinal velocities corresponding to temperatures of a few Kelvin.[62] By combining the filter with a trap, the slow, filtered molecules can be stored.[63]

Pulsed molecular beams are essential for various additional deceleration methods, such as Stark deceleration, Zeeman deceleration, optical deceleration, and various mechanical methods. In a pulsed molecular beam, molecular densities of 10^{13} molecules cm^{-3} can be attained, with translational temperatures near 1 K. The rotational temperature in such a beam generally corresponds to a good approximation to the translational temperature, while the vibrational degrees of freedom are generally known to be cooled significantly less effectively. With a supersonic expansion, molecular packets are produced that are not only cold internally, but in which the molecules also have a very narrow relative velocity distribution; that is, they are very cold within their moving reference system.[64] The absolute velocity of the molecules, however, is referenced to the laboratory system. For molecules within a supersonically expanded packet, the absolute velocity is very high and directed (Figure 5), and depends on the temperature and the pressure of the source and on the mass of the carrier gas employed. If the source is operated at room temperature, the absolute velocity corresponds to 2000 m s^{-1} for helium, 440 m s^{-1} for krypton, and 330 m s^{-1} for xenon.

These pulsed molecular beams are an ideal starting point for an important group of cooling techniques: Stark deceleration, Zeeman deceleration, and optical deceleration. For all three methods, a fraction of the molecules is cut out of the supersonically expanded packet. By exploiting the interaction of the molecule with external fields, this fraction is caused to slow down relative to the coordinate system of the laboratory (Figure 5b). This step is described in greater detail in Section 3.

3. Preparation of Cold Molecules Starting with Molecular Beams

3.1. Stark Deceleration

The method of Stark deceleration[65–67] is quite well established, and has been utilized for slowing down a series of polar molecules: metastable CO ($a^3\Pi$),[65] ND_3 and NH_3,[68,66] OH[69–71] and OD,[72] metastable NH ($a^1\Delta$),[73] H_2CO[74] and SO_2[75] in so-called low-field-seeking states, and metastable CO ($a^3\Pi$),[76] OH,[71] YbF,[77] and benzonitrile[78] in high-field-seeking states. Stark deceleration utilizes the Stark effect, which describes the interaction of a polar molecule with an electric field.

In general, a distinction must be made between molecules in states with a positive and a negative Stark effect. In accordance with their behavior in inhomogeneous electric fields, these are also designated as low-field-seeking and high-field-seeking. The ground state of any molecule is high-field-seeking. Molecules in high-field-seeking states lose potential energy with increasing electric field, whereas molecules in low-field-seeking states gain potential energy. Consequently, molecules in high-field-seeking states are attracted by an electric field maximum, and molecules in a low-field-seeking state by a minimum, as their total energy will then be minimized. Moreover, there are also states that have only a

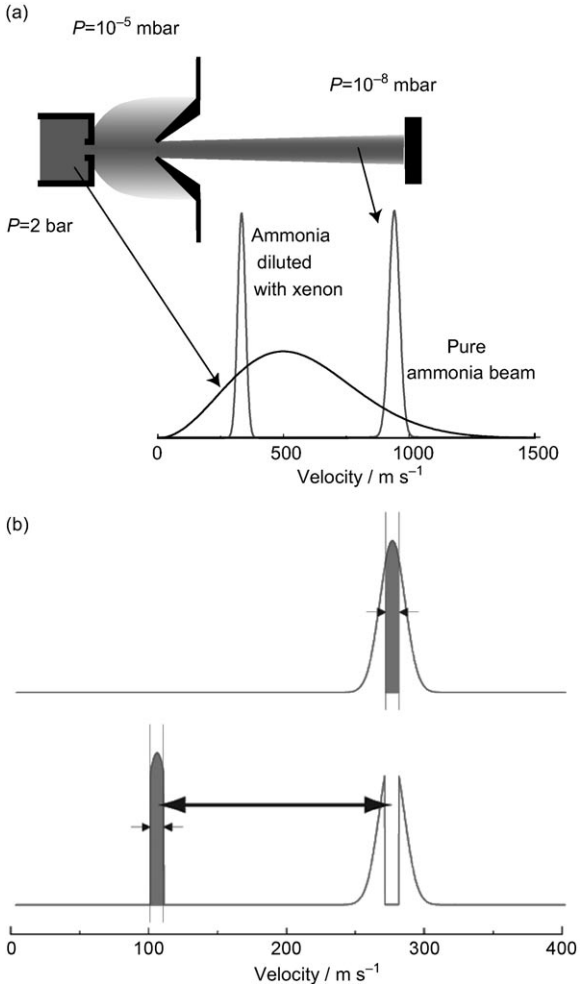

Figure 5. a) The principle of supersonic expansion to generate pulsed molecular beams. A gas is expanded under high pressure from a container through a small hole into a region with significantly lower pressure ($P = 10^{-5}$–10^{-6} mbar). Particles with transverse velocity components that are too high are separated with a skimmer, so that the resulting pulsed molecular beam is highly directed. As is apparent from the velocity distribution for ammonia molecules in a container at room temperature and in the supersonic beam, the molecules in the molecular beam have a narrow velocity distribution (i.e., relative to an accompanying coordinate system they are already very cold), but the absolute velocity of the molecules relative to the laboratory coordinate system is still very high (see text). If a heavy noble gas (e.g. xenon) is used as carrier gas, the absolute velocity is reduced significantly, and the velocity distribution of molecules in the packet is narrower. b) Cooling methods (Section 3) reduce the absolute velocity of the molecules further relative to the laboratory coordinate system by cutting out a part of the molecular packet which is decelerated by interaction with electromagnetic fields.

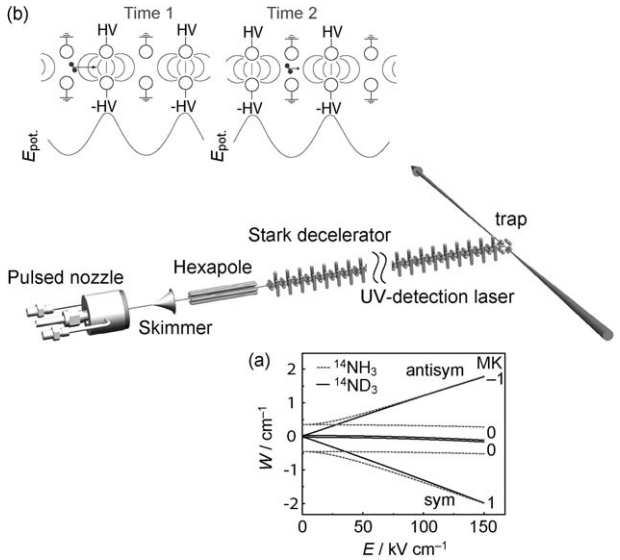

Figure 6. Design of a molecular-beam Stark deceleration experiment. The molecules are expanded through a pulsed nozzle into a vacuum chamber and skimmed. With the aid of an electrostatic hexapole that acts as a positive lens on polar molecules in low-field-seeking states, they are focused onto the entrance of the decelerator (the decelerator is shown in an abbreviated form for clarity; in reality it consists of 96 pairs of electrodes, and is 520 mm long). At the end of the decelerator there may be a molecular trap, a spectroscopy zone, or a storage ring. Finally, the molecules are laser-detected either by laser-induced fluorescence (LIF) or REMPI. The overall setup is about 1 m long. a) Stark effect of the two ammonia isotopologues NH_3 and ND_3. Because of its significantly lower inversion energy ($W_{inv} = 1430$ MHz), $^{14}ND_3$ already shows a dominant linear Stark effect at quite low electric field strengths, whereas $^{14}NH_3$ ($W_{inv} = 23\,694$ MHz) starts to show linear Stark behavior only at field strengths above 50 kV cm^{-1}. b) Operating principle of a Stark decelerator (see text).

very weak Stark effect, such as the $MK = 0$ states of the $|JK> = |11>$ state of the vibronic ground state $\tilde{X}(v=0)$ of ammonia. Figure 6a shows, for example, the Stark effect of the two ammonia isotopologues $^{14}NH_3$ und $^{14}ND_3$.

The operation principle of a Stark decelerator for neutral polar molecules in low-field-seeking states is similar to that of a linear accelerator for charged particles.[65,66] Whereas in accelerators for charged particles the force applied to the particles depends upon the charge of the particle and the electric field, in a Stark decelerator the important quantities are the molecular dipole moment and the gradient of the electric field. This quantum-state-specific force is typically eight orders of magnitude less than the force usually applied to charged particles in an accelerator, but it is still sufficient to influence, and in a targeted way to control, the motion of polar molecules.

In a Stark decelerator, an array of electric fields that are inhomogeneous in the longitudinal direction is used to manipulate the longitudinal velocity of a packet of polar molecules (Figure 6b); that is, their absolute velocity relative to the laboratory system is reduced. For this purpose, the even electrode pairs are set to high voltages at a specific time, whereas the odd pairs are grounded. The diameter of the electrodes is typically 3 mm. The distance between two electrodes within a pair is 2 mm, whereas two electrode pairs are separated by 2.5 mm. Molecules in a low-field-seeking state which move along the molecular beam axis z experience this field as a potential hill, and as a consequence they lose kinetic energy (Figure 6b). Along the molecular beam axis z, the electric field has a maximum between the electrodes, which thus corresponds to the highest point on the potential hill. There, molecules have experienced a maximal loss in kinetic energy. If the molecules would be able to fly out

of the electric field again, they would regain this kinetic energy. In a Stark decelerator, however, the electric fields are switched off such that acceleration is prevented, and the molecules fly on with reduced velocity. In other words, kinetic energy is transformed periodically into Stark (potential) energy. In a diabatic description, the electric field periodically performs work on the molecules, whereby the kinetic energy of the molecules is decreased. High voltage is simultaneously applied to the electrode pairs that were previously grounded, such that the molecules once again find themselves at the foot of a potential hill, and again lose kinetic energy. As this process is repeated many times, the velocity of the molecules can be reduced to any desired value. A Stark decelerator typically consists of about 100 electrode pairs.

The amount of kinetic energy that can be removed per switching stage depends upon the Stark effect of the molecule, the field strength between the electrode pairs, and the exact position of a molecule at the moment the fields are being switched. Computer-controlled high-voltage pulses thus determine the final velocity of a molecule. A second important characteristic of the Stark decelerator is that, just as with particle accelerators, the deceleration process is phase-stable. That means that the process can be described as "trapping" of a molecular packet in a potential minimum that moves ever more slowly.[79] In other words, the deceleration process involves not just a single molecule out of the molecular beam, but all the molecules that at the entrance of the decelerator have positions and velocities within a specific range, the so-called acceptance. Thirdly, it is necessary that during the deceleration process, the molecules stay together in the transverse directions as well. As the electric field between two electrodes of a pair is always lower on the molecular beam axis than at the electrodes, molecules in low-field-seeking states are automatically transversely focused toward the molecular beam axis. Taken together, these three characteristics make it possible to decelerate (or accelerate) a selected fraction of the beam to any desired velocity, thereby keeping it together as a compact packet.

Figure 6 shows a setup of a molecular-beam Stark deceleration experiment. With a decelerator consisting of 100 electrode pairs, the experiment is somewhat more than 1 m long. Packets of internally cold molecules are generated using a pulsed nozzle. These packets move in a highly directed way with high velocity relative to the laboratory coordinate system. With the aid of a skimmer, molecules having components of transverse velocity that are too large are separated. Moreover, in this way a differential pumping stage is generated that guarantees a high vacuum (10^{-8}–10^{-9} mbar) in the second section of the experiment. The molecules pass an electrostatic hexapole that acts like a positive lens on molecules in low-field-seeking states, focusing them onto the entrance of the decelerator. In the Stark decelerator, a fraction of the original molecular packet will be decelerated in a computer-controlled and phase-stable fashion to the desired velocity. After leaving the decelerator, the decelerated molecules are either utilized directly for experiments, or directed toward one of several devices, such as traps (Figure 6) or storage rings. Depending upon the type of molecule, detection of the molecules is accomplished by spectroscopic means, such as resonance-enhanced multiphoton ionization (REMPI) or laser-induced fluorescence (LIF). Some of the applications of decelerated and stored molecules are elaborated in Section 6.

An important characteristic of Stark deceleration is that it generates spatially well-defined packets of cold molecules, all of which are in a single specific quantum state. This state selectivity provides an important basis for follow-up experiments, such as high-resolution spectroscopy for precision measurements (Section 6.1), or novel collision experiments at low temperatures (Section 6.3). However, Stark deceleration can also be used for separating nuclear-spin isomers, as illustrated below with the example of *ortho*- and *para*-ND_3.

Figure 7 shows a part of the energy-level diagram for *ortho*- and *para*-ND_3. There is no interconversion of the two nuclear spin isomers on the timescale of a molecular beam

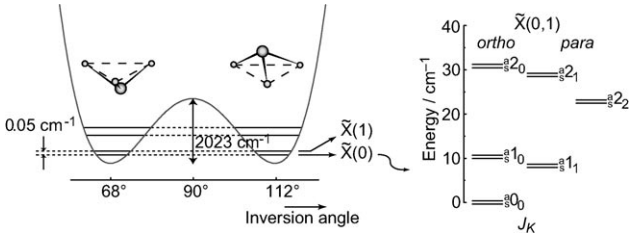

Figure 7. Rotational energy level diagram for *ortho*- and *para*-ND_3 in the vibronic ground state. States with $K=0$ are traditionally denoted as *ortho*-ND_3 and states with $K=1$ as *para*-ND_3. Because of inversion tunneling motion of the ammonia molecule, the rotational levels are split.

experiment, so that it appears as if the sample contains two different molecules in spectroscopic experiments. The deceleration process is controlled such that only molecules in the $|JK>=|11>$ state (*para*-ND_3), which display linear Stark behavior, are selected and decelerated in a phase-stable manner. As states of *ortho*-ND_3 with $K=0$ show only a very small Stark shift, and are therefore barely influenced by electric fields, they are not decelerated in a controlled way, but instead experience alternating small accelerations and decelerations. Thus, they exit the decelerator, together with the carrier gas, with nearly unchanged longitudinal velocity. The phase-stably decelerated molecular packets of *para*-ND_3 in the $|JK>=|11>$ state are therefore separated from *ortho*-ND_3 and can be loaded into an electrostatic trap (see Section 4). If sufficiently long observation times were available it should even be possible to determine the rate of the spontaneous transition of *para*-ND_3 into *ortho*-ND_3. Previous experiments toward the separation of nuclear-spin isomers and measurement of rates of *ortho–para* transformation for CH_3F are described in a highly recommendable review article.[80]

Stark deceleration of molecules in high-field-seeking states, and thus also in molecular ground states, is generally similar to the principles described above for molecules in low-field-seeking states. However, dynamic transverse focusing is

necessary, which complicates the process; for this reason, Section 5 is devoted to the manipulation of molecules in high-field-seeking states.

Stark deceleration of molecules in Rydberg states is a special case. Owing to their strongly delocalized Rydberg electron, these molecules have gigantic dipole moments of several thousand Debyes, so that one pair of electrodes usually suffices for their deceleration.[81,82] However, energy level crossings limit the magnitude of the electric field strength that can actually be used. Pioneering work in this area was carried out with H_2 molecules[83] and argon atoms.[81] Using a Rydberg decelerator, it was possible to stop hydrogen atoms and trap them in two[84] and finally in three[85] dimensions. However, the generally short lifetimes of excited Rydberg states fundamentally limit their possible storage and thus observation time. However, if fluorescence to the ground state is the dominant decay process, cold samples of molecules in the ground state could be obtained in this way. As all atoms and molecules can be excited to Rydberg states, Rydberg deceleration might thereby constitute a quite general method for obtaining samples of cold atoms and molecules in the ground state.

3.2. Zeeman Deceleration

Inspired in part by the use of electric fields to manipulate polar molecules, a magnetic analogue of the Stark decelerator was recently developed for paramagnetic species (Figure 8a). The magnetic interaction (the Zeeman effect) allows the manipulation of a broad range of atoms and molecules to which Stark deceleration cannot be applied. However, for a long time, the necessary rapid switching of high magnetic fields posed a serious experimental challenge. Zeeman deceleration was first demonstrated experimentally in 2007 with hydrogen and deuterium atoms in the ground state, using initially six[86,87] and later twelve[88,89] pulsed stages of magnetic fields. The deceleration stages consisted of 7.8 mm long magnets of insulated copper wire in which magnetic fields of up to 1.5 T could be achieved. The coil design generated a cylindrically symmetric force that, in the transverse direction, focused the molecules back onto the molecular beam axis. By switching on and off the current through the coils, rise and fall times of as little as 5 μs could be achieved. These experiments demonstrate that magnetic fields can now be switched rapidly and precisely enough to permit phase-stable deceleration of neutral particles. Using 64 stages, it has subsequently been possible to Zeeman-decelerate metastable neon atoms[90] and O_2 molecules down to 50 $m\,s^{-1}$.[91]

3.3. Optical Deceleration

The use of optical fields leads to a very general method for manipulating the motion of neutral particles. An intense optical field can polarize molecules and orient them.[92,93] In a laser focus, on the other hand, polarized molecules experience a force proportional to the gradient of the laser intensity. This effect can be used to focus the molecules and to trap them,

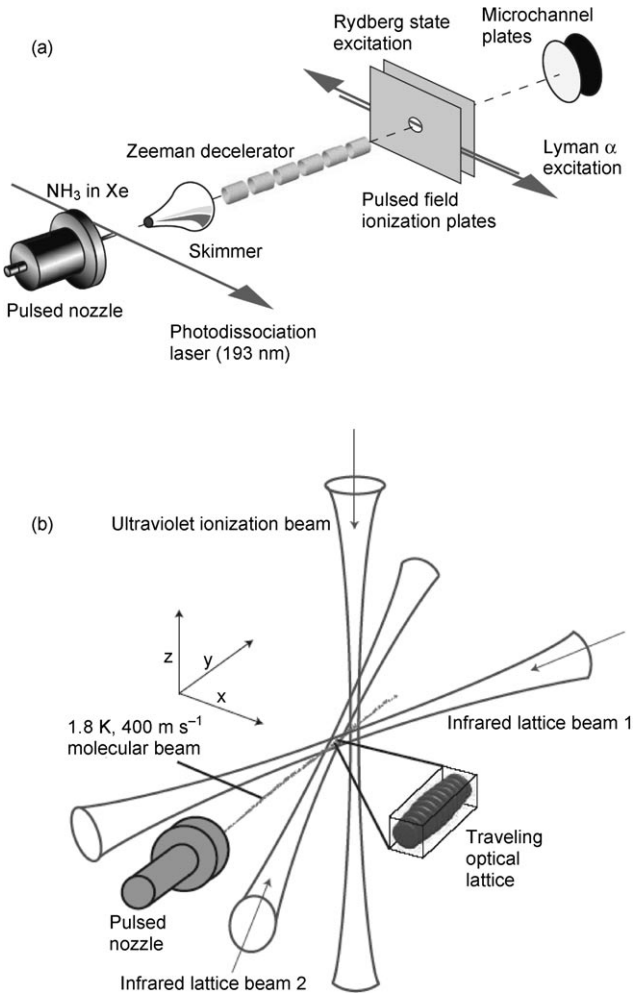

Figure 8. Experimental setups for a) Zeeman deceleration, and b) optical deceleration. In both experiments, the molecules to be cooled are expanded through a pulsed nozzle. The deceleration occurs in (a) with the aid of switched magnetic fields, and in (b) through an ever more slowly moving optical lattice. (Reproduced with permission from Ref. [163]).

and has been demonstrated experimentally by focusing[94] and deflecting[95] a beam of CS_2 molecules with the aid of very intense pulsed laser beams. The force that optical fields exert on molecules has also been employed to decelerate neutral, nonpolar particles:[96] the velocity of benzene molecules was reduced from 320 $m\,s^{-1}$ to 295 $m\,s^{-1}$, and the carrier gas xenon was simultaneously decelerated from 320 $m\,s^{-1}$ to 310 $m\,s^{-1}$.

Significantly larger forces can be achieved if, instead of a single laser beam, two laser beams with nearly opposing directions are used. These two laser beams interfere and form an optical lattice, which represents a periodic array of potential minima for polarizable atoms and molecules (Figure 8b). By carefully controlling the frequency difference between the two lasers, the lattice can be adjusted such that it moves with the same velocity as the molecules in the pulsed molecular beam. Upon gradually reducing the lattice velocity, the molecules themselves can be decelerated to the desired velocity.[97] In a very similar experiment, the velocity of NO

radicals was reduced by 50% with a single laser pulse 5.8 ns long.[98]

As previously noted, phase stability is ensured in Stark and Zeeman deceleration by repeatedly switching back and forth between two static field configurations, whereby the molecules are confined in an energy minimum that *effectively* moves. This concept is fundamentally different from optical decelerators, in which potential minima *actually* move. Recently, deceleration of polar molecules was demonstrated with actually moving potential minima close to the surface of a microstructured array of electrodes.[99]

3.4. Additional Methods

There are other methods for producing cold molecules that also start with pulsed molecular beams but are not based on the interaction of electromagnetic fields with molecules. In an assembly of crossed or opposing molecular beams, the change in kinetic energy owing to collisions[100] or reactions[101] between molecules can be utilized to produce cold molecules or molecules at complete standstill. For example, NO molecules were decelerated to 15 $m s^{-1}$ through billiard-ball-like collisions with argon.[100] Quite recently, an exothermic reaction between opposed beams of potassium atoms and HBr molecules was used to produce slow, and thus translationally cold, KBr molecules.[101]

Moon and co-workers studied mechanical methods for accelerating a molecular beam in the 1970s.[102] Based on this work, a backwards-rotating nozzle was developed with which the laboratory velocity of a molecular beam can be reduced.[103,104] Another mechanical approach is based on backwards-rotating silicon paddles. This concept was actually demonstrated with a Si(111)-H(1×1) crystal mounted on the tip of a rotor, from which atoms or molecules are reflected elastically.[105] With the aid of a rotating helical velocity selector, slow molecules can also be mechanically filtered out from an effusive beam.[106] This method is especially suited for very large molecules of several thousand atomic mass units (amu).

4. Traps for Neutral Molecules

To store cold molecular packets, traps are used. The molecules are trapped by taking advantage of their interaction with an external electromagnetic field, which can be either magnetic, optical, or electric. Paramagnetic molecules in a low-field-seeking state can be trapped owing to the Zeeman effect in a field minimum of a static quadrupole magnetic field. As it is possible to generate strong magnetic fields of several Tesla, traps can be created in this way that are several Kelvin deep. Magnetic fields are often combined with the method of buffer-gas cooling (Section 2).[58] Another possibility is confining the molecules in the focus of an intense laser beam. However, these optical traps are very small (they extend only over the focus volume of the laser beam), and are only a few mK deep.[107,108] On the other hand, they can also be used for trapping non-polar molecules. Moreover, the modest depth is not a disadvantage with very cold molecules, such as those created by photoassociation and at Feshbach resonances, for which they offer a broad variety of applications.

Electric traps are very well suited for the storage of polar neutral molecules.[68,109] For example, decelerated molecules in low-field-seeking states can be loaded into an electrostatic trap right after leaving the decelerator, and stored there for several seconds. As the Stark effect is a property of the respective quantum state, only a single quantum state is stored, which has advantages not only for the investigation of trapped molecules, but also for their subsequent utilization (see also Section 6). Electrostatic traps with a field minimum at the center are very well suited for trapping decelerated polar molecules in low-field-seeking states. These are described in more detail in the following section.

4.1. Electrostatic Traps for Neutral, Polar Molecules in Low-Field-Seeking States

Trapping of polar molecules with the aid of electrostatic fields was first demonstrated in 2000 with decelerated ND_3 molecules.[68] The first electrostatic trap for polar molecules consisted of a quadrupole geometry (Figure 9), as originally suggested by Wing for Rydberg atoms.[109] Electrostatic traps for polar molecules in low-field-seeking states have several advantages: they are usually rather deep (up to 1 K), are of macroscopic dimensions, which facilitates the manipulation and detection of trapped molecules, and they are very versatile.[68,109,110] Although quadrupole traps are the most common, electrostatic fields also allow to generate traps of a more special design, such as hexapole traps, or traps with a double minimum potential.[110]

Figure 9a shows the principle behind the first electrostatic quadrupole trap. It consists of a ring electrode with two end caps.[68] For trapping, potentials are applied to the electrodes (Figure 9a, right) such that the field is zero in the center of the trap. Molecules in low-field-seeking states experience an increase of the electric field strength in every direction such that they are focused back to the trap center and remain stored. The right-hand part of Figure 9b shows the Stark energy of the OH radical in its low-field-seeking $X^2\Pi_{3/2}, J = 3/2$ state as a function of position along the molecular beam axis. Instead of trapping the molecules at a specific position, they can also be stored in a minimum along a ring. In the simplest case, such a storage ring can be conceived by bending an electrostatic hexapole into a torus.[111–113]

For optimal storage of the molecules, a loading stage is incorporated between deceleration and trapping (Figure 9a, left). The decelerated molecular packets experience a last potential hill (Figure 9a, left) as they fly into the trap, which removes their residual kinetic energy so that they come to a standstill right in the center of the trap. The next step involves switching to the trapping configuration. Figure 9c shows a typical time-of-flight measurement for OD radicals ($X^2\Pi_{3/2}$, $J = 3/2$), which are first decelerated to a low velocity (about 20 $m s^{-1}$). After leaving the Stark decelerator they are loaded into an electrostatic quadrupole trap, where they are then stored.

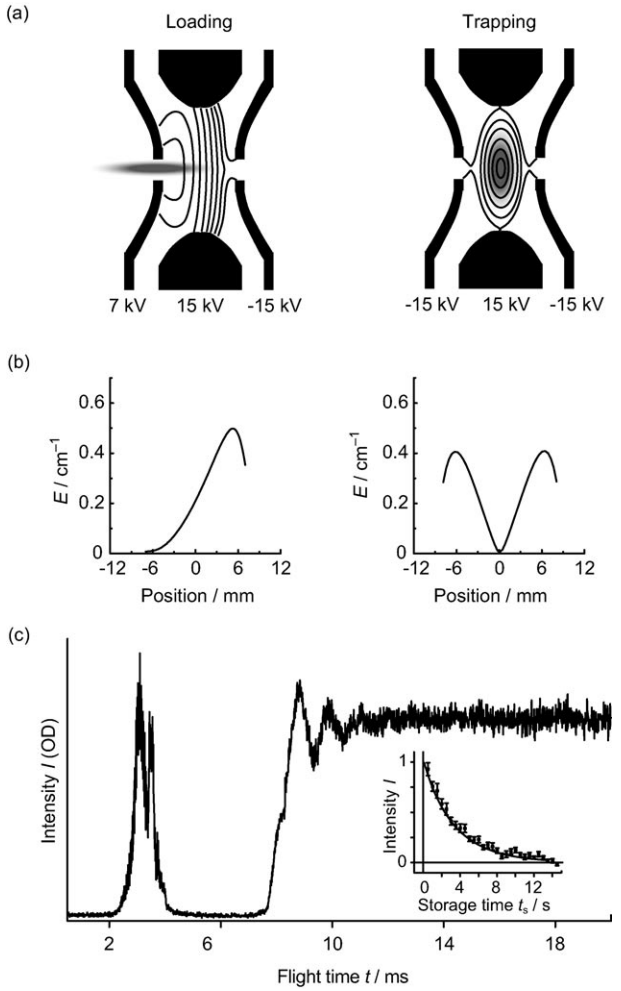

Figure 9. Principle of an electrostatic quadrupole trap. a) Field distribution in the electrostatic quadrupole trap for the loading (left) and trapping configurations (right), as well as the corresponding potentials. Equifield lines are shown, and the behavior and magnitude of the molecular packets are indicated. b) Stark energy of OH radicals along the molecular beam axes for the loading (left) and trapping configurations (right). (Reproduced from Ref. [67,164]). c) Time-of-flight spectrum for OD radicals, which were first decelerated to 20 m s^{-1}, then brought to a standstill in the center of the trap, and finally loaded into an electrostatic quadrupole trap. After initial oscillations in the potential minimum of the trap, the signal from the trapped molecules remains stable. The inset shows the intensity I of OD radicals as a function of storage time t_s, and emphasizes the long trap lifetimes that can be achieved (reproduced with permission from Ref. [72]).

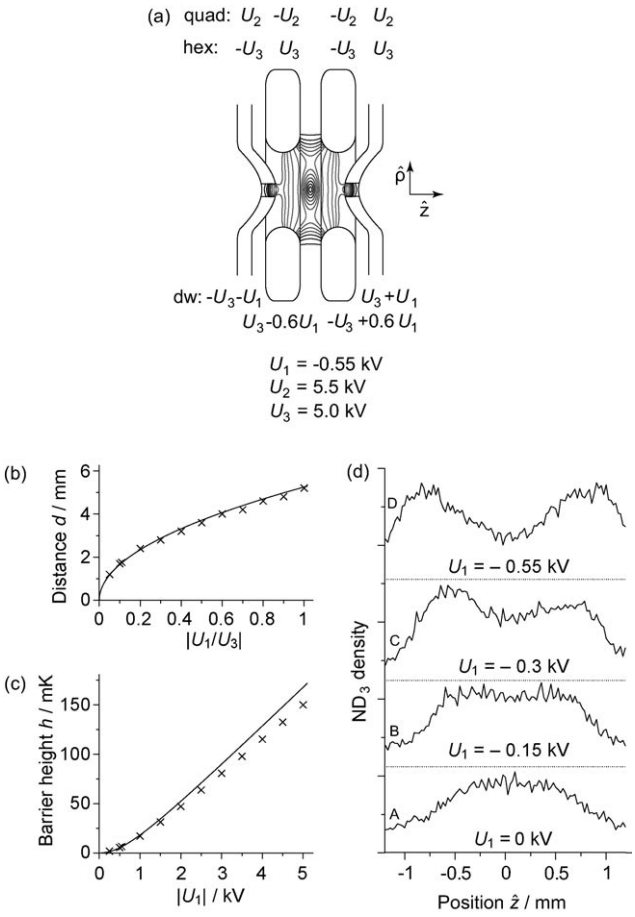

Figure 10. Extended electrostatic trap.[110] a) Representation of the extended trap geometry with the corresponding potentials required for generating a quadrupole (quad, U_2), hexapole (hex, U_3), or double-well trap (dw, U_1 and U_3). b) Dependence of the distance d between the two minima in the double-well trap on the ratio $|U_1/U_3|$. c) Barrier height h as a function of U_1. In (b) and (c), the lines represent the theoretically ideal case, whereas the crosses are based on electric field simulations that use the actual geometry. d) Experimentally determined distribution of trapped ND_3 molecules along the z axis for various U_1 values.

As noted above, one of the advantages of electrostatic traps is their versatility. Figure 10 shows an extension of the classical quadrupole trap with an additional ring electrode. Depending on the applied potentials, this trap geometry can function as quadrupole, hexapole, or double-minimum trap, and thus be adapted to various applications.[110] Double-minimum traps have proven to be very useful for experiments in atomic physics. For example, they have been used for interference experiments in which the coherence properties of a Bose–Einstein condensate[114] were investigated. Another application involved experiments for studying collisions between packets of atoms separated in the two minima after switching to a different trap configuration.[115]

With the arrangement described here, a double-minimum potential trap can be created through a combination of a hexapole field and a dipole field. For a constant hexapole voltage U_3, both the distance between the two minima and the height of the barrier in the double-minimum trap depend only on the magnitude of the dipole field, and thus on U_1, so that they can easily be adjusted (Figure 10b and c).

This effect is also visible experimentally. Figure 10d shows the experimentally determined distribution of molecules along the molecular beam axis z for various values of U_1. Curve A shows the density distribution of molecules in the hexapole trap along the z direction with $U_3 = 5.5$ kV. In the next step, a dipole field is added ($U_1 = -0.15$ kV, curve B); the distribution becomes broader. With increasing size of the dipole field and a constant hexapole contribution, a readily apparent double-minimum structure develops, in which, as

predicted theoretically, both the distance between the two minima and the height of the barrier between the minima are dependent upon the magnitude of the dipole contribution (Figure 10d, curves C and D).

In principle, this behavior can be exploited for new types of collision experiments between cold molecular packets: molecules would initially be stored in the double-minimum trap, and two separate packets would form. By switching to the hexapole configuration, the double-minimum structure would collapse. The molecules then have a potential energy corresponding to the height of the former barrier, and they are accelerated toward the new trap minimum at the center, where they collide. To date, however, the density of trapped molecules actually achieved has not been sufficient to permit a study of such collisions.

4.2. Trap Losses

There exist at least three fundamental mechanisms for the loss of trapped molecules, namely collisions, black-body radiation, and non-adiabatic transitions, and these will be briefly introduced in what follows. An important source of loss is collisions with background gas; that is, particles which are still present in the vacuum chamber, but which have not been trapped. If these warm, and thus fast, particles collide with the cold, trapped molecules, the latter gain kinetic energy and are subsequently kicked out of the trap. Losses owing to collisions with background gas can be minimized by establishing better vacuum conditions. In another scenario, trapped molecules change quantum states through inelastic collisions with each other, so that they may no longer remain trapped. Losses of this sort play an important role for molecule ensembles created at Feshbach resonances or through photoassociations, as very high densities of molecules are achieved here: 10^{13}–10^{15} molecules per cubic centimeter or more (see Section 2). With the far lower densities obtained through Stark deceleration combined with electrostatic trapping (10^{7}–10^{8} molecules cm^{-3}), this loss mechanism plays essentially no role.

Black-body radiation, which is present everywhere, also contributes to trap losses. Polar molecules generally have strong vibrational and rotational transitions in the infrared region of the spectrum, and can therefore be pumped into another untrapped state by black-body radiation at room temperature. Transitions via black-body radiation therefore represent a fundamental limitation on the lifetime of trapped polar molecules. In a recent study, Hoekstra et al. investigated the influence of black-body radiation on trapped OH radicals. The $1/e$ capture time for OH and OD (both in the $X^2\Pi_{3/2}, v = 0, J = 3/2(f)$ state) is limited to 2.8 or 7.1 seconds, respectively, at 298 K through transitions to non-trapped rotational states caused by black-body radiation.[72] Losses from black-body radiation can be reduced either by lowering the temperature of the experimental setup to liquid nitrogen temperature, for example, or by careful choice of the molecule to be studied. The trap lifetime due to black-body radiation ranges from only 0.61 s for LiH to over 1000 s for the two alkali metal dimers RbCs and KRb.[72]

Another loss mechanism results from non-adiabatic transitions, which are also known as Majorana transitions. These can arise in a typical quadrupole trap, for example, which has zero electric field at its center (Figure 9). For many molecules, a state degeneracy can arise under field-free conditions, such as for the $MK = -1$ and $MK = 0$ states of the ammonia molecule (see Figure 6a), so that trapped molecules in the $MK = -1$ state can undergo a transition to the non-trapped $MK = 0$ state. Non-adiabatic transitions can be suppressed with traps that have a sufficiently high, non-zero electric field at the trap center. Such traps were first realized for static magnetic fields, and are known as Ioffe–Pritchard (IP) traps.[116,117] In atomic physics, the use of traps that prevent non-adiabatic transitions were a key step toward the first Bose–Einstein condensate of atoms, because only then trap losses through non-adiabatic transitions could be avoided.[2,3]

Very recently, an electrostatic analogue of an IP trap for polar molecules was also built and demonstrated.[118] The trap geometry consists of six electrodes. Depending on the voltages applied, both a trap with a non-zero electric field minimum at the center, so that non-adiabatic losses are inhibited, and a trap with a zero-field trap minimum can be created with the same trap geometry. By a direct comparison of trap lifetimes of $^{14}ND_3$ molecules in these two trap configurations it could be shown that in the trap with zero field at its center the density of molecules decreased significantly more rapidly, which could be attributed to non-adiabatic transitions. Furthermore, from the trap lifetimes of the four ammonia isotopologues $^{14}NH_3$, $^{15}NH_3$, $^{14}ND_3$, and $^{15}ND_3$, it could be shown that the losses that are due to non-adiabatic transitions depend strongly on the precise energy-level structure of the molecules.[118]

A similar trap was also demonstrated for Rydberg atoms.[85] In this case as well, atoms remained stored in the trap noticeably longer than for a zero-field trap. The capture time for the hydrogen Rydberg atoms investigated was 135 μs, and thus limited only by the fluorescence lifetime of the trapped $n = 30$, $k = 25$, $m = 0$ Stark state.

5. Deceleration and Trapping Of Molecules in High-Field-Seeking States

As the ground states of all molecules are high-field-seeking, as are all states for larger, heavier molecules, there is great interest in controlling and manipulating the motion of molecules in high-field-seeking states as well. However, this is much more difficult than with low-field seekers, as the maximum of an electric field is always localized at the electrodes. Unlike molecules in low-field-seeking states, it thus becomes necessary to prevent molecules in high-field-seeking states from being accelerated too strongly towards the electrodes, and then actually colliding with them. This is accomplished with alternating gradient (AG) deceleration, in which, in addition to the actual deceleration process, the molecules are also dynamically focused in the transverse directions.[76] A detailed description of AG deceleration is given in a Review.[119] In view of the applications in precision

measurements described in Section 6 for decelerated molecules, cold molecules in high-field-seeking states are especially interesting, as both the effect of parity violation in chiral molecules and that of the permanent electric dipole moment of the electron increases, and thus becomes easier to detect, when heavy atoms are present in the molecule.

To trap molecules in high-field-seeking states, it is again necessary to employ time-dependent fields. This was first demonstrated successfully with so-called alternating current (AC) traps,[120] in which trapping is achieved by switching back and forth between different saddle-point configurations for the electric field, as described in detail in Section 5.2. Optical or microwave fields have also been proposed as traps for molecules in high-field-seeking states. Molecules in high-field-seeking states have already been trapped at the focus of a CO_2 laser beam.[107,108] In the proposed microwave trap, polar molecules in high-field-seeking states would be trapped in a maximum of a standing microwave field.[121]

5.1. AG Deceleration

In principle, the method for decelerating molecules in high-field-seeking states is similar to that for molecules in low-field-seeking states. However, the molecules are no longer decelerated when they fly into an inhomogeneous electric field, but when they fly out. As already noted, this is complicated by the deflection of the molecules toward the electrodes, where the electric field has a maximum. To inhibit the molecules from colliding with the electrodes, the molecules are dynamically focused in the transverse directions. A representation of an AG decelerator is shown in Figure 11 a. In contrast to a Stark decelerator (Figure 6), the electrode pairs are not oriented perpendicular to the molecular beam axis z, but parallel to it. If, when the field is turned on, a molecular packet is between the electrodes in the first pair of electrodes, molecules in a high-field-seeking state will experience a focusing force in the y direction, because the field decreases with increasing distance from the molecular beam axis z, and a defocusing force in the x direction, because the electric field increases toward the electrodes. Up to ± 15 kV may be applied to the individual electrode pairs. The next pair of electrodes is located in the yz plane, and is thus rotated by 90° around the molecular beam axis relative to the preceding pair. This time, molecules in high-field-seeking states are therefore focused in the x direction and defocused in the y direction. The decreasing field at the ends of the electrodes (fringe fields) is used for deceleration (Figure 11 b).

Stable deceleration of molecules in high-field-seeking states is possible because the magnitude of the force on a molecule in the transverse direction increases with its distance from the molecular beam axis as long as the molecule has not moved too far away from this axis. Molecules that are focused toward the molecular beam axis in one transverse direction thus experience a weaker force when the fields are switched to the defocusing force in that particular transverse direction. With the right switching frequency, there is therefore always an overall focusing force in the transverse direction acting on high-field seekers. The method of AG deceleration has so far been applied to CO in its metastable $a^3\Pi$ state,[76] the OH radical,[71] the heavy-atom molecule YbF,[77] and the large molecule benzonitrile C_7H_5N,[78] whereby the kinetic energy of benzonitrile has been reduced by 18% and that of OH by 21%.

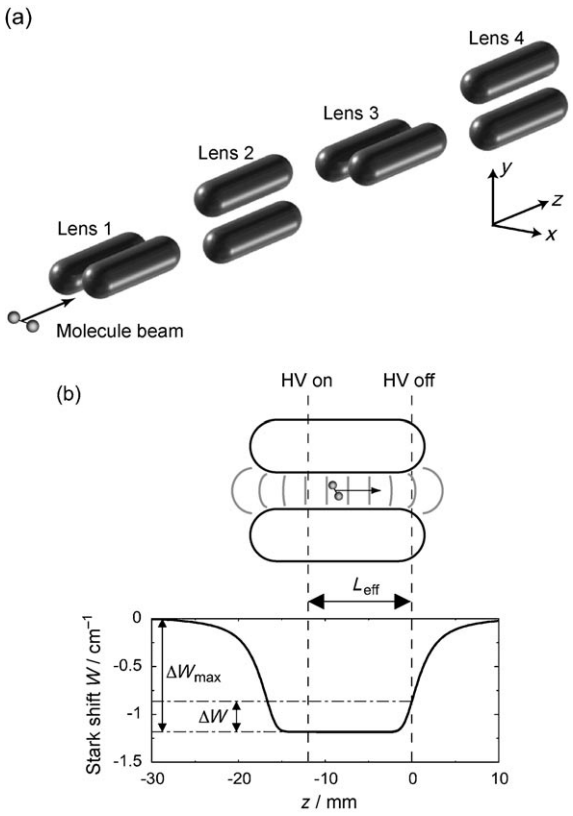

Figure 11. Principle of AG deceleration. a) Representation of the first four stages in an AG decelerator. In contrast to an ordinary Stark decelerator, the electrode pairs are oriented parallel to the z axis in an AG decelerator for high-field-seeking molecules. To guarantee dynamic, transverse focusing, the orientation of the electrode pairs alternate in the xz and the yz planes. Electrodes within a pair are 20 mm long, have a diameter of 6 mm, and are 2 mm apart. Each electrode pair is used to both focus and decelerate the molecules. b) Simplified representation of the electric field between the two electrodes of a pair (top), and the resulting Stark energy W along the molecular beam axis z for CO molecules in the metastable $a^3\Pi$, $J=1$, $\Omega=1$, $M\Omega=+1$ level (bottom) if the potential difference for the pair of electrodes is 20 kV. The way in which the electric fields are switched on and off during AG deceleration to achieve both focusing in the transverse direction and deceleration in the longitudinal direction is also shown. (Reproduced from Ref. [119]).

5.2. AC Traps

To trap high-field seekers, a maximum in the electric field would be required. According to Earnshaw's theorem, it is not possible to create a three-dimensional field maximum in free space using electrostatic fields; however, the creation of a saddle point of the electric field with a field minimum in one direction and a field maximum in the other two directions is possible. By rapid switching between two or three field

configurations with mutually orthogonal saddle points, molecules in high-field-seeking states can be dynamically trapped. Traps for high-field seekers thus take advantage of a principle similar to that of an AG decelerator, albeit now applied with respect to the time domain and no longer with respect to the molecular beam axis z. AC traps for neutral polar molecules in high-field-seeking states are equivalent to Paul traps for charged particles, which were implemented as early as 1955.[122,123]

There are three trap geometries that permit the formation of orthogonal saddle points: linear traps, cylindrically symmetric traps, and three-phase traps (Figure 12).[124] In the case

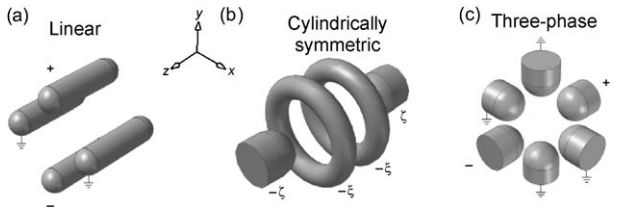

Figure 12. The three possible AC trap geometries: a) linear, b) cylindrically symmetric, and c) with three phases. (Reproduced from Ref. [124]).

of molecules, the cylindrically symmetric[120,124] and linear traps[125,126] have already been implemented and trapping has been demonstrated, whereas for atoms that are always high-field-seeking, both cylindrically symmetric[127] and three-phase traps[128] have been used. The AC trap principle will be explained here using the example of a linear AC trap (Figure 13). The trap is located directly behind the decelerator, so that the decelerated molecular packet can be loaded optimally into the trap, and it consists of four double

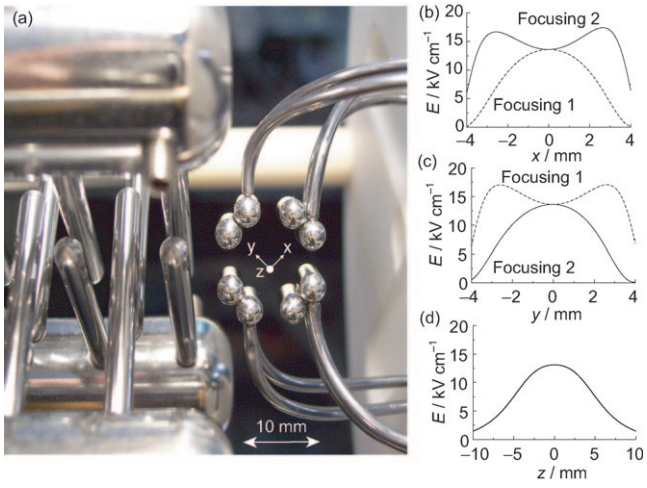

Figure 13. a) Linear AC trap consisting of four double electrodes arranged in a quadrupolar manner. b–d) Electric field strength for the two switching configurations of the electric field in the b) x, c) y, and d) z directions. The linear AC trap is located very close to the exit of the decelerator, which is visible in the left part of the photograph, so that the trap can be loaded very effectively. (Reproduced from Ref. [125]).

electrodes arranged in a quadrupolar manner.[125] If a potential of up to ± 10 kV is applied to the two electrodes along the y axis (Figure 13), and the two along the x axis remain grounded, a saddle point with a maximum along the x and z directions and a minimum along the y direction (focusing 1) is formed. Molecules in high-field-seeking states are therefore focused along x and z, and defocused along y. When a potential is applied to the opposing electrodes along the x axis, and the two along the y axis remain grounded, a saddle point rotated by 90° is formed (focusing 2). High-field seekers are therefore focused along y and z and simultaneously defocused along x. By switching between these two saddle-point configurations, molecules in high-field-seeking states experience alternately focusing and defocusing forces along x and y (Figure 13b,c), whereas the force along z is unaffected by the switching, and always remains focusing (Figure 13d).

Figure 14 shows the dependence of the density of trapped $^{15}ND_3$ molecules on the switching frequency in a cylindrically symmetric AC trap (Figure 12b). This trap is suited to

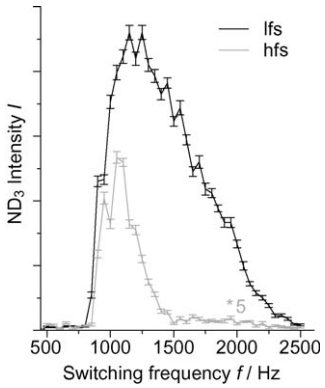

Figure 14. Frequency dependence of the trapping efficiency of the cylindrically symmetric AC trap for $^{15}ND_3$ molecules in high-field-seeking (hfs) and low-field-seeking (lfs) states. The intensity for the molecules in high-field-seeking states is scaled by a factor of 5 to compensate for the reduced number of molecules that are loaded into the trap.

trapping molecules both in low-field- and in high-field-seeking states.[120,124] In both cases, no molecules remain trapped for low switching frequencies; the molecules are defocused or focused, respectively, for so long that they leave the trap. A significant increase in trapped molecules begins at 900 Hz. The region over which molecules can be trapped passes through a maximum, and then decreases again at higher frequencies, as the trap becomes shallower with increasing switching frequency. In the stable trapping region, which is dependent both on the trapped molecules and upon the applied high voltages, resonances of molecular motion with the switching frequency of the electric field can occur, which leads to a decrease in the density of trapped molecules. The stability of AC traps can be described in analogous fashion to ion traps and mass filters using the stability parameters a and q and a stability diagram.[126] A

variety of additional experiments for the characterization of AC molecule traps have been performed and are discussed in detail elsewhere.[124]

6. Applications of Cold Molecules

The creation of cold molecular packets, and thus the control over the motion and orientation of the molecules through external fields, offers a variety of new possibilities for precision studies of molecular properties and interactions. In recent years, several experiments demonstrating these possibilities have been suggested and conducted. These experiments can be divided into four groups: spectroscopic studies, conformer separation and orientation, molecular beam collision experiments, and experiments with trapped molecules.

6.1. High-Resolution Spectroscopy and Precision Measurements

Ultimately, the resolution in every spectroscopic experiment is limited by the interaction time of the particles under investigation with the radiation field. In conventional molecular beam experiments, this interaction time usually is a few hundred microseconds. The ability to produce slow, intense molecular beams significantly increases the attainable interaction time in the spectroscopic experiment, and thus the resolution.

Thus, one logical application of decelerated molecular packets is to use them in spectroscopic experiments to gain increased resolution. The setup and results for a prototypical spectroscopic experiment with cold molecules are presented in Figure 15. $^{15}ND_3$ molecules are decelerated with a Stark decelerator to 100 m s^{-1} and 52 m s^{-1}. Then they pass through a transversally focusing hexapole before encountering a 6.5 cm long homogeneous microwave zone.[8] In this way, the hyperfine structure for the inversion transition of $^{15}ND_3$ was determined for the first time. It is clearly apparent that with decreasing velocity of the molecules, and thus longer exposure time in the microwave zone, the resolution increases: Curve a in Figure 15 shows the hyperfine spectrum recorded for $^{15}ND_3$ at a molecular velocity of 280 m s^{-1}; that is, when the molecules have not been subjected to extra deceleration. The spectrum in curve b was taken with molecules decelerated to 52 m s^{-1}. In curve c, the microwave power was lowered in addition to reduce the effects of power broadening. Curves d–f are enlargements of a detail of spectra a–c. At a molecular velocity of 280 m s^{-1} (curve d), the doublet structure at 1430.515 MHz is not yet resolved, but it is readily observable with slow molecular packets (100 m s^{-1}

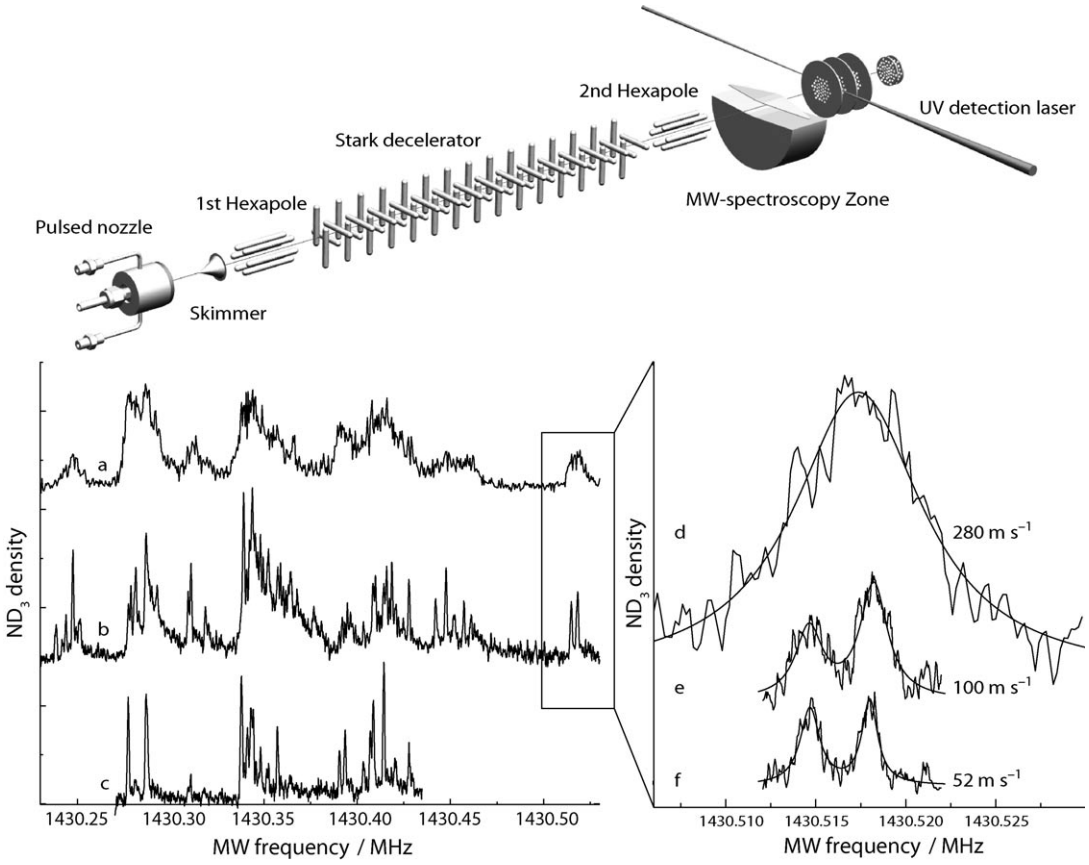

Figure 15. Experimental setup and measurement of the hyperfine structure of the $^{15}ND_3$ inversion transition. The Stark decelerator is shown in abbreviated form. Curves a and b show the complete spectra for the two molecule velocities 280 m s^{-1} and 52 m s^{-1}. Curve c was recorded with 52 m s^{-1} slow molecules, but using reduced microwave power compared with curve b. Curves d–f are excerpts from the complete spectra, and emphasize the increase in resolution for slower molecules.[8]

(curve e) and 52 m s^{-1} (curve f)). Altogether, it was possible to determine all 22 hyperfine levels with a precision of better than 100 Hz.

In a similar experiment, Hudson et al.[9] were able to spectroscopically study decelerated OH radicals in the $^2\Pi_{3/2}$ rovibronic ground state. It was possible to determine the frequencies of the $\Delta F = \pm 1$ satellite lines of OH with tenfold greater precision than previously achieved. Among other things, these results are relevant for astrophysical studies.

A spectroscopy zone can generally be combined quite easily with both a Stark or AG decelerator and with other sources of cold molecules, and thus utilized for spectroscopic experiments with previously unprecedented resolution. The resolution can be improved through use of a longer interaction zone and/or even slower molecules, especially in molecular fountains. In a new type of molecular fountain experiment currently being constructed at the Laser Center of the Free University of Amsterdam,[129] polar molecules are to be initially decelerated to a few meters per second, then cooled, and subsequently shot upward. The molecules fly up for about 30 cm before falling down again under gravity. In the process they pass twice through a microwave cavity. The effective observation time in this Ramsey-like arrangement encompasses the overall flight time between the two passages through the cavity, so that very long observation times of about 0.5 s are attainable.[129]

A major research branch in modern physics involves the search for effects beyond the so-called standard model of particle physics, such as changes in the values of the fundamental constants of nature as a function of time, for example the fine-structure constants $\alpha = e^2/4\pi\varepsilon_0\hbar c$,[15,16] or the ratio of proton mass to that of the electron $\mu = m_p/m_e$,[17,18] that are predicted by cosmological models. There are astrophysical observations that indicate changes in natural constants in earlier epochs of the universe. As the astrophysical data are controversially discussed, it is important to carry out high-precision laboratory experiments concerning these questions. Very recently it proved possible, through a combination of results from high-precision spectroscopic measurements on H_2 in the laboratory with very precise spectral lines for the H_2 molecule in quasars, to determine a change in the mass ratio $\mu = m_p/m_e$ of $\Delta\mu/\mu = (2.4 \pm 0.6) \times 10^{-5}$.[17] This result suggests that μ may have decreased in the past 12×10^9 years.

Other interesting phenomena beyond the standard model that have been predicted but have not yet been verified owing to their minuteness, include parity violations in chiral molecules [10–13] and the permanent electric dipole moment of the electron.[14] Both effects have in common that they are larger and thus easier to detect for molecules containing large, heavy atoms. All the states of molecules with large, heavy atoms are high-field-seeking. To exploit the long observation times of cold, polar molecules for precision measurements, AG deceleration (Section 5.1) must be utilized. Polar molecules are especially suited for such measurements because the presence of an external electric field leads to a greatly intensified internal field and thus an enhancement of the effect.[14] For example, efforts are currently being made to sufficiently decelerate the YbF molecule with the aim to determine the permanent electric dipole moment of the electron.[14,77]

6.2. Conformer Separation and Orientation

Recently, a method analogous to AC traps was used to accomplish a selector for high-field seekers.[130] This method made it possible to demonstrate a clear separation of the two conformers of 3-aminophenol (*cis*- und *trans*-3-aminophenol) on the basis of their different mass-to-dipole moment ratios. In principle, the selector corresponds to a quadrupole mass filter for ions that separates species on the basis of their mass-to-charge ratios. For a given AC switching frequency, the two conformers experience different focusing forces, resulting in differing transmissions through the selector.[130] These experiments show that molecular packets containing only a single conformer can be generated, and then made available for novel investigations of relatively large (bio)molecules in the gas phase.

In another experiment, the combination of a strong electrostatic field together with laser fields was used to first align samples of state-selected iodobenzene molecules in one dimension, and then in a subsequent experiment to orient them.[131] In the strong, inhomogeneous electrostatic field of a deflector, the original supersonic beam of polar molecules, which are present in multiple rotational states and also in several vibrational states (see also Section 2), was split up spatially as a function of their state-specific dipole moments. Molecules in the lowest rotational state have the highest dipole moment, and are therefore most strongly deflected spatially. This way, they can be selectively used for further experiments, independent of the remaining of the molecular beam. In the experiment described, the resulting state-selected samples permitted a previously unachieved level of alignment ($\langle\cos^2\theta_{2D}\rangle = 0.97$), as well as a high degree of orientation. Such selection and orientation experiments with pure samples of polar ground-state molecules promise novel experimental possibilities for chemistry, for example in structure determination or for the study of the conformer selectivity in chemical reactions.

6.3. Investigations of Cold Collisions, and Prospects for Cold Chemistry

The lowest temperature in interstellar space is approximately 2.76 K. In dense interstellar clouds, reactions in cold atom–molecule systems in the gas phase play a key role. If cold atoms and molecules could be simultaneously stored in traps with sufficiently high density, important reaction parameters could be studied in the laboratory. The standard method to date for investigating reactions at low temperature is the CRESU technique,[132] which is based on a simultaneous isentropic expansion of the reactants along with helium buffer gas through a Laval nozzle. This permits the study of the temperature dependence of reactions down to 13 K. The strength of the CRESU technique lies in the nature of the isentropic expansion of the gas, which achieves a gas flow that

is uniform with respect to temperature, density, and velocity. The relatively high density in the expansion (10^{16}–10^{18} cm^{-3}) ensures that thermal equilibrium is maintained at all times,[133] in contrast to pulsed molecular beams, with which no thermal equilibrium is established, and for which it is thus impossible to define a single temperature at a specific location in the beam.

The low kinetic energy of cold molecules results in very large translational De Broglie wavelengths relative to the particle size. Whereas the De Broglie wavelength of ammonia at room temperature is, for example, about 23 pm, and thus approximately one third of the classical distance between the atoms in the molecule, it has already risen to circa 2.5 nm at a kinetic energy of 25 mK. At a kinetic energy of 1 mK it amounts to roughly 10 nm for molecules, and thus exceeds significantly the diameter of smaller molecules. As a result of the large De Broglie wavelength, even collisions between large molecules still show a significant quantum effect in this temperature range; that is, they can no longer be regarded as collisions between two hard spheres but rather as interference between two waves, which can be constructive as well as destructive in nature. The large De Broglie wavelengths of cold molecules can therefore completely change the nature of reaction dynamics.

Furthermore, the low kinetic energy of cold molecules is often insufficient to overcome the activation energy for chemical reactions on a potential energy surface. Instead, tunneling processes through these energy barriers gain importance, and in fact become the dominant reaction pathways. For example, the simple reaction $F + H_2 \rightarrow HF + H$ is hindered by a substantial energy barrier of 7 $kJ\,mol^{-1}$. Theoretical studies predict, however, that at very low temperatures, the reaction will be accelerated by tunneling processes. The calculated rate constant is $k = 1.25 \times 10^{-12}$ $cm^3\,s^{-1}$ for $T \approx 0$ K.[134]

Recent theoretical[22,23] and experimental[24,25] studies have shown that in general, chemical reaction processes at low temperatures are very efficient. According to Wigner,[135] for reactions near absolute zero, the cross-section for elastic collisions (σ_{el}) and for reactions (σ_r) behave as $\sigma_{el} \sim v^{4l}$ and $\sigma_r \sim v^{2l-1}$ in the limiting case of vanishing collision velocity v, where l is the angular momentum of the colliding molecules. At very low temperature, both σ_{el} and σ_r are dominated by $l = 0$ (s-wave character). It follows that the elastic collision cross-section σ_{el} is independent of the collision energy, whereas the reaction cross-section σ_r behaves inversely proportional to the velocity. At vanishingly low velocity v, the reaction cross-section σ_r therefore approaches infinity ($\sigma_r \rightarrow \infty$ for $v \rightarrow 0$). Moreover, long-range interactions become increasingly important as reaction entrance channels. Interesting effects for reactions at temperatures near absolute zero can therefore be anticipated. Cold molecules thus open up novel possibilities for investigating chemical reaction dynamics in a new, previously inaccessible regime.

For elementary chemical reactions, the coupling of various degrees of freedom (translation, rotation, and inter- and intramolecular vibration) is of great importance. Since the first experiments, which concentrated on the dynamics of chemical reactions,[136] the efforts of many researchers have been concentrated on achieving external control over chemical reactions. This goal has stimulated rapid development in the field of coherent control of molecular processes,[137] optimal control of molecular dynamics,[138–140] and stereochemistry.[141] Many excellent experiments have demonstrated the possibility of controlling unimolecular reactions with laser fields, such as molecular decay or isomerization, or selective bond breaking.[137,140] External control of bimolecular reactions is made more difficult by thermal motion of the molecules, as this leads to random orientations of the reaction partners when they collide, thus minimizing the effect of external fields on molecular collisions. Thermal motion can be reduced by cooling the gases employed to low temperatures. Electromagnetic fields can therefore significantly influence molecular collisions, and thus the course of the reaction, only if the translational energy of the molecules is less than the interaction energy with the external fields. With the static electric and magnetic fields currently achievable experimentally (up to 150 $kV\,cm^{-1}$ or 5 T), molecular energy levels can be displaced by a few Kelvin, so external control of molecular dynamics in the gas phase should be possible at temperatures below 1 K.[142] In other words, with the development of techniques for attaining cold polar molecules in the mK temperature region, the possibility of controlling bimolecular processes with external fields has come into reach.[74] However, an experimental demonstration and application is still to be achieved.

It is striking that chemical reactions under ultracold conditions ($T < 1$ mK) in a trap will proceed differently depending upon whether the reaction products are fermions or bosons,[143] as the possible product states with respect to rotation, vibration, and translation are fully quantized. If the reaction products are fermions, then they must obey the Pauli principle, which states that two fermions cannot be identical in all quantum numbers. This is referred to as Pauli blocking,[144] and leads to an appreciable effect only at ultracold temperatures, because at higher temperatures, the number of possible product states is very large. With bosons, on the other hand, there are no restrictions regarding the occupation of individual states. In fact, it can be demonstrated that the reaction rate of a process into an already occupied state can be enhanced. This effect is known as Bose enhancement or Bose stimulation.[144]

Apart from unimolecular processes, a collision between potential reaction partners is the fundamental prerequisite for a chemical reaction. Collisions between molecules are heavily dependent upon the relative velocities of the colliding partners. Especially with low collision velocities, the formation of relatively long-lived collision complexes is possible. These are also referred to as resonances, as the kinetic energies of the molecules are comparable to energy separations between rotational energy levels in the collision complex. In this case, translational energy is converted into rotational energy, which leads to a transient binding of the molecules. Long-lived collision complexes occur at well-defined collision velocities of the two reacting partners, and show up as sharp maxima (resonances) in the collision-energy dependence of the collision cross-sections.[23,26,27] It becomes clear from theoretical studies that resonances can have a

drastic effect on chemical reactions at low temperatures. It is difficult, however, to experimentally observe the occurrence of resonances in collisions between two molecules, because in most experiments, the kinetic energies of the associated molecules are distributed over a wide range.

Owing to the narrow velocity distribution of the decelerated molecules, their precisely adjustable kinetic energies, and their quantum state selectivity, Stark decelerated molecular beams are extremely well-suited to collision experiments involving crossed molecular beams, as was recently demonstrated with the example of a Stark decelerated OH beam scattered with a conventional xenon atom beam.[145] By changing the kinetic energy of the OH radicals, it was possible to vary the collision energy over the threshold energy values for various collision channels, so that the threshold behavior of the inelastic collision cross-sections could be determined precisely. Even lower collision energies and a higher energy resolution can be achieved if two Stark decelerated molecular beams crossing at a 90° angle are employed. For this purpose, a new experiment is currently being set up at the Fritz Haber Institute with which it will be possible to study inelastic and reactive collisions of two different molecules as a function of the collision energy, with a collision energy resolution of better than 1 cm^{-1}.

Another broad field of cold chemistry is concerned with collisions and reactions between ions and molecules. Two current experiments will serve here as examples. Quite recently, a novel experiment[146] was performed in which cold reactive collisions between laser-cooled ions trapped in a linear Paul trap and velocity-selected neutral polar molecules (see Section 2) were investigated, using the example of the strongly exothermic reaction of Ca^+ with CH_3F (Figure 16). This technique is a general approach to studying reactive collisions between ions and polar molecules over a broad temperature range. It was possible to achieve collision energies of $\bar{E}_{Collision}/k_b \geq 1$ K and single-particle sensitivity.

In another experiment, the temperature dependence of the simple proton-transfer reaction[147] $NH_2^- + H_2 \rightarrow NH_3 + H^-$, which is slightly exothermic, was investigated. The reaction was carried out in a 22-pole radio-frequency trap for ions in which the NH_2^- ions were stored. The trapped anions were thermalized by collisions with helium buffer gas introduced into the housing for the trap. The trap temperature could be varied between 8 and 300 K. The reaction is initiated and controlled by adding hydrogen to the helium buffer gas. The measured rate constant shows an inverse temperature dependence up to 20 K, where it reaches a maximum;[147] with further temperature increase the rate constant decreases again. The inverse temperature behavior can be understood qualitatively with a statistical model, which assumes a dynamic bottleneck that hinders the formation of an intermediate reaction complex. At low temperatures, the quantum behavior of the system must however be taken into account. The appearance of a maximum value for the reaction probability may suggest a resonance. It will be of interest to see whether a similar behavior will be observed for other reactions once further investigations at low temperatures are performed.

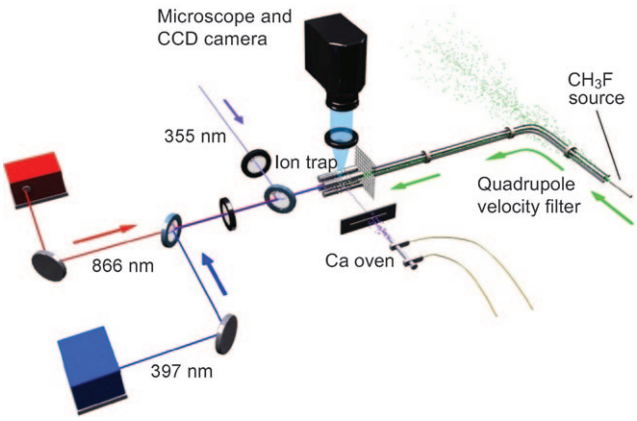

Figure 16. Experimental setup for a collision experiment between trapped Ca^+ ions and velocity-selected polar CH_3F molecules.[146] (Reproduced with permission from Ref. [146]).

6.4. Applications of Trapped Molecules

6.4.1. Determining the Lifetimes of Excited States

Trapped molecules can be studied for several seconds. It is however difficult to utilize the potentially long interaction time of the trapped molecules with electromagnetic radiation directly for high-resolution spectroscopy, because the molecules interact with the inhomogeneous trapping field, and complex effects, such as line splitting and line shifts, can considerably complicate a precise spectroscopic analysis. Nevertheless, it could be shown that trapped molecules are ideally suited to precisely determine the lifetimes of metastable states. The lifetimes of vibrationally excited states typically lie in the region of milliseconds to seconds, and thus outside the observation times that are normally available in ordinary molecular-beam gas-phase experiments. Only the direct determination of lifetimes as short as a few milliseconds has been possible.[148] Complex experimental procedures were developed to permit the indirect determination of long lifetimes.[149,150] Such experimental limitations have contributed to the fact that ab initio calculations have gained increasing importance with respect to these questions. However, deviations between the results of indirect experimental determinations and theoretical values can amount to as much as 50%.[21] As observation times of several seconds are possible with trapped molecules, lifetimes of excited states can be determined directly. This was first demonstrated with OH radicals stored in an electrostatic quadrupole trap. It was possible to precisely determine the lifetime of the first excited vibrational state $X^2\Pi$, $v = 1$ and thus also to establish a new reference value for the Einstein A coefficient in the important Meinel system.[19,151] For the determination of the lifetime, Stark decelerated OH radicals in the vibrational ground state ($v = 0$, $J = 3/2$) and in the first excited vibrational state ($v = 1$, $J = 3/2$) were trapped in an electrostatic trap under otherwise identical experimental conditions, and their density was measured as a function of trapping time.[19] The results are presented in Figure 17. The trap lifetime for the $v = 1$ state is significantly shorter than that for the $v = 0$ state. By compar-

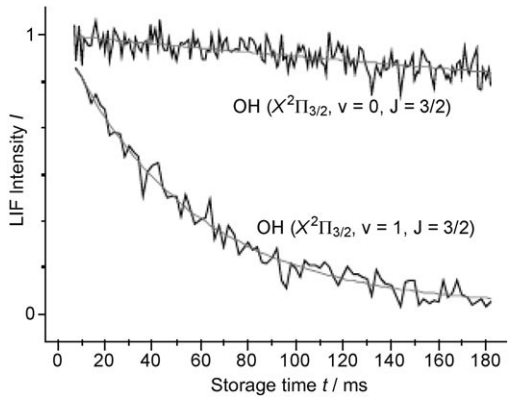

Figure 17. Direct determination of the lifetime of the first excited vibrational state $v=1$ of the electronic ground state of the OH radical.[19] The lifetime of the long-lived excited state can be determined directly from comparative measurements of the storage time t of the $v=1$ and the $v=0$ states in an electrostatic quadrupole trap. LIF = laser-induced fluorescence. (Reproduced from Ref. [19]).

ing the two curves, the lifetime of the excited vibrational state $v=1$ can be determined directly to be (59.0 ± 2.0) ms, with considerably greater precision than before.[19]

The lifetime of specific excited states of CO[20] could also be determined by means of Stark deceleration and subsequent storage in an electrostatic quadrupole trap, whereas the lifetime of vibrationally excited NH[21] could be determined with the aid of buffer gas cooling (see Section 2) and subsequent storage in a magnetic quadupole trap could clarify existing uncertainties about their precise magnitudes.

6.4.2. *Phenomena at Very Low Temperatures*

The ability to store molecules in traps promises further developments in the field of ultracold molecules. At sufficiently low temperatures, the De Broglie wavelength is comparable to or even greater than the distance between the individual particles in a packet. In this realm, quantum degenerate effects dominate the dynamics of molecules, and a Bose–Einstein condensate can be formed. It has been predicted theoretically that the anisotropic, long-range dipole–dipole interactions between cold polar molecules will lead to a new and rich physics in these cold, dipolar gases.[152–154] First hints came through the formation of a Bose–Einstein condensate of chromium atoms with magnetic dipole–dipole interactions.[155,156] Very strong interactions are present between electric dipoles; these strong electric dipole–dipole interactions between cold polar molecules also promise interesting prospects for various schemes for quantum computing.[157,158]

To be able to study such phenomena, the temperature of the trapped polar molecules must be lowered even more and the density increased. So far, various cooling procedures have been suggested with which it should be possible to reach temperatures below 1 mK. The most promising methods are evaporative cooling, in which the warmest among an ensemble of trapped molecules are removed selectively, followed by rethermalization of the molecules, and sympathetic cooling, where trapped molecules are brought in contact with an ultracold atom gas, and a new thermal equilibrium is established with the aid of elastic collisions. Another cooling method that has been discussed for the preparation of molecular packets with temperatures below 1 mK is cavity-assisted laser cooling.[159–161]

Trap losses through inelastic collisions that transfer molecules out of the trapped low-field-seeking state into a non-trapped high-field-seeking state are regarded as a serious problem for the first two cooling methods. AC traps, such as those described in Section 5.2, which can store molecules in high-field-seeking states and thus in the ground state, are an important approach to circumvent this problem. However, the densities achieved to date with AC-trapped molecules are still too low. It is also suspected that the micromotions that the trapped molecules undergo in AC traps as a result of the switched fields might complicate reaching the very low temperatures that are required.

A very promising approach would be to transfer molecules at a sufficiently low temperature into, for example, an optical trap that is also appropriate for molecules in high-field-seeking states, and in which micromotions like those in AC traps would not occur. In this way it should in principle be possible to reach very low temperatures; that is, the ultracold regime for directly cooled molecules.

7. Summary and Prospects

Research on cold molecules is developing at a feverish pace. Cold molecules offer perspectives as exciting as that of ultracold atoms, but the preparation of such molecules is challenging, because laser cooling that is so successful for atoms fails completely. Nevertheless, in the last few years, several methods have been developed for the preparation of cold molecules (see Table 1). Of special interest for chemists are direct cooling techniques that begin with the molecules to be cooled, as they are applicable to more complex and often chemically more interesting molecules, in contrast to approaches that start with atoms that are already ultracold.

A series of methods is based on pulsed molecular beams that generate packets with internally cold molecules having a very narrow relative velocity distribution. The Stark decelerator has proven to be very successful. It functions as an inverse linear accelerator, and uses the Stark effect to decelerate electrically neutral, polar molecules. These slow molecules can then either be utilized directly, for example in spectroscopic experiments, or they are injected into a storage ring or stored in molecule traps with customized properties. Apart from the manipulation of polar molecules in low-field-seeking states, it has also been possible in recent years to decelerate molecules in high-field-seeking states using the AG principle. These can then be stored in AC traps. Both the states of larger and heavier molecules and the ground states of all molecules are high-field-seeking. Because larger and heavier molecules can play an important role in precision measurements, and the ground states are required for evaporative cooling and for sympathetic cooling, which are key steps on the way toward a Bose–Einstein condensate

from polar molecules, it is especially interesting to achieve complete control over molecules in high-field-seeking states.

The great interest in cold molecules has been stimulated by the prospect of new applications, and the potential for fundamental discoveries. Table 1 shows that the majority of the experimental studies have been limited to simple molecular systems to date. For chemical applications, however, it would also be interesting to develop sources of more complex cold molecules. The combination of AG deceleration and corresponding molecule traps is very promising for the generation of very cold samples of larger (bio)molecules. For very large molecules up to 6000 amu, mechanical processes appear primarily suited.

Apart from intensive efforts in the generation of colder and denser molecular packets, various applications for cold molecules have been developed in the meantime: high-resolution spectroscopy and precision measurements, measurements of lifetimes for long-lived excited states, and investigations of (ultra)cold chemistry and low-temperature phenomena.

An important step in the investigation of (ultra)cold chemistry is an understanding of collisions in this temperature regime, which differ fundamentally from those at room temperature. Collision experiments between slow hydroxyl radicals and xenon atoms have recently provided interesting first insight into scattering processes at low velocity, and constitute an interesting step in the direction of ultracold chemistry. Interesting and novel effects are predicted for chemistry in the ultracold region, including the dominance of tunneling processes, which lead to very large reaction cross-sections in the vicinity of absolute zero. However, these effects still await experimental verification: a true terra incognita to be explored.

Many of the experiments described herein were carried out in the Department of Molecular Physics at the Fritz-Haber-Institut by a large group of students, postdocs, and technicians, whom we wish to thank. M.S. thanks the Fonds der Chemischen Industrie for a Liebig Fellowship. The authors also thank the anonymous reviewers for their comments and suggestions.

Received: November 11, 2008

Translated by Prof. William Russey, Laconia, New Hampshire

[1] S. Bose, *Z. Phys.* **1924**, *26*, 178 – 181.
[2] E. A. Cornell, C. E. Wieman, *Rev. Mod. Phys.* **2002**, *74*, 875 – 893.
[3] W. Ketterle, *Rev. Mod. Phys.* **2002**, *74*, 1131 – 1151.
[4] W. Ketterle, *ChemPhysChem* **2002**, *3*, 736 – 753.
[5] "Passion for Precision (Einstein lecture)": T. W. Hänsch, *Ann. Phys.* **2006**, *15*, 627 – 652.
[6] H. J. Metcalf, P. van der Straten, *Laser Cooling and Trapping*, Springer, New York, **1999**.
[7] *Low Temperatures and Cold Molecules* (Ed.: I. W. M. Smith), Imperial College Press, London, **2008**.
[8] J. van Veldhoven, J. Küpper, H. L. Bethlem, B. Sartakov, A. J. A. van Roij, G. Meijer, *Eur. Phys. J. D* **2004**, *31*, 337 – 349.
[9] E. R. Hudson, H. J. Lewandowski, B. C. Sawyer, J. Ye, *Phys. Rev. Lett.* **2006**, *96*, 143004.
[10] M. Quack, *Angew. Chem.* **2002**, *114*, 4812 – 4825; *Angew. Chem. Int. Ed.* **2002**, *41*, 4618 – 4630.
[11] M. Quack, J. Stohner, *Chirality* **2001**, *13*, 745 – 753.
[12] P. Schwerdtfeger, R. Bast, *J. Am. Chem. Soc.* **2004**, *126*, 1652 – 1653.
[13] J. Crassous, C. Chardonnet, T. Saue, P. Schwerdtfeger, *Org. Biomol. Chem.* **2005**, *3*, 2218 – 2224.
[14] J. J. Hudson, B. E. Sauer, M. R. Tarbutt, E. A. Hinds, *Phys. Rev. Lett.* **2002**, *89*, 023003.
[15] J. K. Webb, M. T. Murphy, V. V. Flambaum, V. A. Dzuba, J. D. Barrow, C. W. Churchill, J. X. Prochaska, A. M. Wolfe, *Phys. Rev. Lett.* **2001**, *87*, 091301.
[16] R. Srianand, H. Chand, P. Petitjean, B. Aracil, *Phys. Rev. Lett.* **2004**, *92*, 121302.
[17] E. Reinhold, R. Buning, U. Hollenstein, A. Ivanchik, P. Petitjean, W. Ubachs, *Phys. Rev. Lett.* **2006**, *96*, 151101.
[18] A. Shelkovnikov, R. J. Butcher, C. Chardonnet, A. Amy-Klein, *Phys. Rev. Lett.* **2008**, *100*, 150801.
[19] S. Y. T. van de Meerakker, N. Vanhaecke, M. P. J. van der Loo, G. C. Groenenboom, G. Meijer, *Phys. Rev. Lett.* **2005**, *95*, 013003.
[20] J. J. Gilijamse, S. Hoekstra, S. A. Meek, M. Metsaelae, S. Y. T. van de Meerakker, G. Meijer, G. C. Groenenboom, *J. Chem. Phys.* **2007**, *127*, 221102.
[21] W. C. Campbell, G. C. Groenenboom, H.-I. Lu, E. Tsikata, J. M. Doyle, *Phys. Rev. Lett.* **2008**, *100*, 083003.
[22] P. F. Weck, N. Balakrishnan, *Int. Rev. Phys. Chem.* **2006**, *25*, 283 – 311.
[23] J. M. Hutson, P. Soldan, *Int. Rev. Phys. Chem.* **2006**, *25*, 497 – 526.
[24] P. Staanum, S. D. Kraft, J. Lange, R. Wester, M. Weidemüller, *Phys. Rev. Lett.* **2006**, *96*, 023201.
[25] N. Zahzam, T. Vogt, M. Mudrich, D. Comparat, P. Pillet, *Phys. Rev. Lett.* **2006**, *96*, 023202.
[26] N. Balakrishnan, A. Dalgarno, *J. Chem. Phys.* **2000**, *113*, 621 – 627.
[27] E. Bodo, F. A. Gianturco, *Int. Rev. Phys. Chem.* **2006**, *25*, 313 – 351.
[28] J. Weiner, V. S. Bagnato, S. Zilio, P. S. Julienne, *Rev. Mod. Phys.* **1999**, *71*, 1 – 85.
[29] F. Masnou-Seeuws, P. Pillet, *Adv. Atom. Mol. Opt. Phys.* **2001**, *47*, 53 – 127.
[30] W. C. Stwalley, H. Wang, *J. Mol. Spectrosc.* **1999**, *195*, 194 – 228.
[31] K. M. Jones, E. Tiesinga, P. D. Lett, P. S. Julienne, *Rev. Mod. Phys.* **2006**, *78*, 483 – 535.
[32] T. Köhler, K. Góral, P. S. Julienne, *Rev. Mod. Phys.* **2006**, *78*, 1311 – 1361.
[33] C. Chin, R. Grimm, P. Julienne, E. Tiesinga, *Rev. Mod. Phys.* **2009**, arXiv:0812.1496.
[34] H. R. Thorsheim, J. Weiner, P. S. Julienne, *Phys. Rev. Lett.* **1987**, *58*, 2420 – 2423.
[35] P. D. Lett, K. Helmerson, W. D. Phillips, L. P. Ratliff, S. L. Rolston, M. E. Wagshul, *Phys. Rev. Lett.* **1993**, *71*, 2200 – 2203.
[36] J. D. Miller, R. A. Cline, D. J. Heinzen, *Phys. Rev. Lett.* **1993**, *71*, 2204 – 2207.
[37] J. Hecker Denschlag, H.-C. Nägerl, R. Grimm, *Phys. J.* **2004**, *3*, 33 – 39.
[38] D. Kleppner, *Phys. Today* **2004**, *57*, 12 – 13.
[39] P. Courteille, R. S. Freeland, D. J. Heinzen, F. A. van Abeelen, B. J. Verhaar, *Phys. Rev. Lett.* **1998**, *81*, 69 – 72.
[40] T. Kraemer, M. Mark, P. Waldburger, J. G. Danzl, C. Chin, B. Engeser, A. D. Lange, K. Pilch, A. Jaakkola, H. C. Nägerl, R. Grimm, *Nature* **2006**, *440*, 315 – 318.
[41] M. Greiner, C. A. Regal, D. S. Jin, *Nature* **2003**, *426*, 537 – 540.

[42] S. Jochim, M. Bartenstein, A. Altmeyer, G. Hendl, S. Riedl, C. Chin, J. Hecker Denschlag, R. Grimm, *Science* **2003**, *302*, 2101 – 2103.
[43] M. W. Zwierlein, C. A. Stan, C. H. Schunck, S. M. F. Raupach, S. Gupta, Z. Hadzibabic, W. Ketterle, *Phys. Rev. Lett.* **2003**, *91*, 250401.
[44] I. Bloch, J. Dalibard, W. Zwerger, *Rev. Mod. Phys.* **2008**, *80*, 885 – 964.
[45] J. M. Sage, S. Sainis, T. Bergeman, D. DeMille, *Phys. Rev. Lett.* **2005**, *94*, 203001.
[46] J. Deiglmayr, A. Grochola, M. Repp, K. Mörtlbauer, C. Glück, J. Lange, O. Dulieu, R. Wester, M. Weidemüller, *Phys. Rev. Lett.* **2008**, *101*, 133004.
[47] M. Viteau, A. Chotia, M. Allegrini, N. Bouloufa, O. Dulieu, D. Comparat, P. Pillet, *Science* **2008**, *321*, 232 – 234.
[48] K.-K. Ni, S. Ospelkaus, M. H. G. de Miranda, A. Péer, B. Neyenhuis, J. J. Zirbel, S. Kotochigova, P. S. Julienne, D. S. Jin, J. Ye, *Science* **2008**, *322*, 231 – 235.
[49] F. Lang, K. Winkler, C. Strauss, R. Grimm, J. Hecker Denschlag, *Phys. Rev. Lett.* **2008**, *101*, 133005.
[50] N. V. Vitanov, T. Halfmann, B. W. Shore, K. Bergmann, *Annu. Rev. Phys. Chem.* **2001**, *52*, 763 – 809.
[51] J. G. Danzl, E. Haller, M. Gustavsson, M. J. Mark, R. Hart, N. Bouloufa, O. Dulieu, H. Ritsch, H.-C. Nagerl, *Science* **2008**, *321*, 1062 – 1066.
[52] J. Küpper, J. M. Merritt, *Int. Rev. Phys. Chem.* **2007**, *26*, 249 – 287.
[53] M. Y. Choi, G. E. Douberly, T. M. Falconer, W. K. Lewis, C. M. Lindsay, J. M. Merritt, P. L. Stiles, R. E. Miller, *Int. Rev. Phys. Chem.* **2006**, *25*, 15 – 75.
[54] F. Stienkemeier, K. K. Lehmann, *J. Phys. B* **2006**, *39*, R127 – R166.
[55] J. P. Toennies, A. F. Vilesov, *Angew. Chem.* **2004**, *116*, 2674 – 2702; *Angew. Chem. Int. Ed.* **2004**, *43*, 2622 – 2648.
[56] "The study of cold collisions using ion guides and traps": D. Gerlich in *Low Temperatures and Cold Molecules* (Ed.: I. W. M. Smith), Imperial College Press, London, **2008**, pp. 121 – 174.
[57] "The production and study of ultra-cold molecular ions": D. Gerlich in *Low Temperatures and Cold Molecules* (Ed.: I. W. M. Smith), Imperial College Press, London, **2008**, pp. 295 – 344.
[58] J. D. Weinstein, R. deCarvalho, T. Guillet, B. Friedrich, J. M. Doyle, *Nature* **1998**, *395*, 148 – 150.
[59] S. E. Maxwell, N. Brahms, R. deCarvalho, D. R. Glenn, J. S. Helton, S. V. Nguyen, D. Patterson, J. Petricka, D. DeMille, J. M. Doyle, *Phys. Rev. Lett.* **2005**, *95*, 173201.
[60] M. Stoll, J. M. Bakker, T. C. Steimle, G. Meijer, A. Peters, *Phys. Rev. A* **2008**, *78*, 032707.
[61] D. Patterson, J. M. Doyle, *J. Chem. Phys.* **2007**, *126*, 154307.
[62] S. A. Rangwala, T. Junglen, T. Rieger, P. W. H. Pinkse, G. Rempe, *Phys. Rev. A* **2003**, *67*, 043406.
[63] T. Junglen, T. Rieger, S. A. Rangwala, P. W. H. Pinkse, G. Rempe, *Phys. Rev. Lett.* **2004**, *92*, 223001.
[64] D. Levy, *Science* **1981**, *214*, 263 – 269.
[65] H. L. Bethlem, G. Berden, G. Meijer, *Phys. Rev. Lett.* **1999**, *83*, 1558 – 1561.
[66] H. L. Bethlem, G. Meijer, *Int. Rev. Phys. Chem.* **2003**, *22*, 73 – 128.
[67] S. Y. T. van de Meerakker, N. Vanhaecke, G. Meijer, *Annu. Rev. Phys. Chem.* **2006**, *57*, 159 – 190.
[68] H. L. Bethlem, G. Berden, F. M. H. Crompvoets, R. T. Jongma, A. J. A. van Roij, G. Meijer, *Nature* **2000**, *406*, 491 – 494.
[69] J. R. Bochinski, E. R. Hudson, H. J. Lewandowski, G. Meijer, J. Ye, *Phys. Rev. Lett.* **2003**, *91*, 243001.
[70] S. Y. T. van de Meerakker, P. H. M. Smeets, N. Vanhaecke, R. T. Jongma, G. Meijer, *Phys. Rev. Lett.* **2005**, *94*, 023004.
[71] K. Wohlfart, F. Filsinger, F. Grätz, J. Küpper, G. Meijer, *Phys. Rev. A* **2008**, *78*, 033421.
[72] S. Hoekstra, J. J. Gilijamse, B. Sartakov, N. Vanhaecke, L. Scharfenberg, S. Y. T. van de Meerakker, G. Meijer, *Phys. Rev. Lett.* **2007**, *98*, 133001.
[73] S. Hoekstra, M. Metsälä, P. C. Zieger, L. Scharfenberg, J. J. Gilijamse, G. Meijer, S. Y. T. van de Meerakker, *Phys. Rev. A* **2007**, *76*, 063408.
[74] E. R. Hudson, C. Ticknor, B. C. Sawyer, C. A. Taatjes, H. J. Lewandowski, J. R. Bochinski, J. L. Bohn, J. Ye, *Phys. Rev. A* **2006**, *73*, 063404.
[75] S. Jung, E. Tiemann, C. Lisdat, *Phys. Rev. A* **2006**, *74*, 040701.
[76] H. L. Bethlem, A. J. A. van Roij, R. T. Jongma, G. Meijer, *Phys. Rev. Lett.* **2002**, *88*, 133003.
[77] M. R. Tarbutt, H. L. Bethlem, J. J. Hudson, V. L. Ryabov, V. A. Ryzhov, B. E. Sauer, G. Meijer, E. A. Hinds, *Phys. Rev. Lett.* **2004**, *92*, 173002.
[78] K. Wohlfart, F. Grätz, F. Filsinger, H. Haak, G. Meijer, J. Küpper, *Phys. Rev. A* **2008**, *77*, 031404.
[79] H. L. Bethlem, G. Berden, A. J. A. van Roij, F. M. H. Crompvoets, G. Meijer, *Phys. Rev. Lett.* **2000**, *84*, 5744 – 5747.
[80] P. L. Chapovsky, L. J. F. Hermans, *Annu. Rev. Phys. Chem.* **1999**, *50*, 315 – 345.
[81] E. Vliegen, H. J. Wörner, T. P. Softley, F. Merkt, *Phys. Rev. Lett.* **2004**, *92*, 033005.
[82] E. Vliegen, F. Merkt, *J. Phys. B* **2005**, *38*, 1623 – 1636.
[83] Y. Yamakita, S. R. Procter, A. L. Goodgame, T. P. Softley, F. Merkt, *J. Chem. Phys.* **2004**, *121*, 1419 – 1431.
[84] E. Vliegen, S. D. Hogan, H. Schmutz, F. Merkt, *Phys. Rev. A* **2007**, *76*, 023405.
[85] S. D. Hogan, F. Merkt, *Phys. Rev. Lett.* **2008**, *100*, 043001.
[86] N. Vanhaecke, U. Meier, M. Andrist, B. H. Meier, F. Merkt, *Phys. Rev. A* **2007**, *75*, 031402.
[87] S. D. Hogan, D. Sprecher, M. Andrist, N. Vanhaecke, F. Merkt, *Phys. Rev. A* **2007**, *76*, 023412.
[88] S. D. Hogan, A. W. Wiederkehr, M. Andrist, H. Schmutz, F. Merkt, *J. Phys. B* **2008**, *41*, 081005.
[89] S. D. Hogan, A. W. Wiederkehr, H. Schmutz, F. Merkt, *Phys. Rev. Lett.* **2008**, *101*, 143001.
[90] E. Narevicius, A. Libson, C. G. Parthey, I. Chavez, J. Narevicius, U. Even, M. G. Raizen, *Phys. Rev. Lett.* **2008**, *100*, 093003.
[91] E. Narevicius, A. Libson, C. G. Parthey, I. Chavez, J. Narevicius, U. Even, Mark G. Raizen, *Phys. Rev. A* **2008**, *77*, 051401.
[92] B. Friedrich, D. Herschbach, *Phys. Rev. Lett.* **1995**, *74*, 4623 – 4626.
[93] H. Stapelfeldt, T. Seideman, *Rev. Mod. Phys.* **2003**, *75*, 543 – 557.
[94] B. S. Zhao, H. S. Chung, K. Cho, S. H. Lee, S. Hwang, J. Yu, Y. H. Ahn, J. Y. Sohn, D. S. Kim, W. K. Kang, D. S. Chung, *Phys. Rev. Lett.* **2000**, *85*, 2705 – 2708.
[95] H. Stapelfeldt, H. Sakai, E. Constant, P. B. Corkum, *Phys. Rev. Lett.* **1997**, *79*, 2787 – 2790.
[96] R. Fulton, A. I. Bishop, P. F. Barker, *Phys. Rev. Lett.* **2004**, *93*, 243004.
[97] P. F. Barker, M. N. Shneider, *Phys. Rev. A* **2002**, *66*, 065402.
[98] R. Fulton, A. I. Bishop, M. N. Shneider, P. F. Barker, *Nat. Phys.* **2006**, *2*, 465 – 468.
[99] S. A. Meek, H. L. Bethlem, H. Conrad, G. Meijer, *Phys. Rev. Lett.* **2008**, *100*, 153003.
[100] M. S. Elioff, J. J. Valentini, D. W. Chandler, *Science* **2003**, *302*, 1940 – 1943.
[101] N.-N. Liu, H. Loesch, *Phys. Rev. Lett.* **2007**, *98*, 103002.
[102] P. B. Moon, C. T. Rettner, J. P. Simons, *J. Chem. Soc. Faraday Trans.* **1978**, *74*, 630 – 643.
[103] M. Gupta, D. Herschbach, *J. Phys. Chem. A* **1999**, *103*, 10670 – 10673.

[104] M. Gupta, D. Herschbach, *J. Phys. Chem. A* **2001**, *105*, 1626 – 1637.
[105] E. Narevicius, A. Libson, M. F. Riedel, C. G. Parthey, I. Chavez, U. Even, M. G. Raizen, *Phys. Rev. Lett.* **2007**, *98*, 103201.
[106] S. Deachapunya, P. J. Fagan, A. G. Major, E. Reiger, H. Ritsch, A. Stefanov, H. Ulbricht, M. Arndt, *Eur. Phys. J. D* **2008**, *46*, 307 – 313.
[107] T. Takekoshi, B. M. Patterson, R. J. Knize, *Phys. Rev. Lett.* **1998**, *81*, 5105 – 5108.
[108] E. R. Hudson, N. B. Gilfoy, S. Kotochigova, J. M. Sage, D. DeMille, *Phys. Rev. Lett.* **2008**, *100*, 203201.
[109] W. H. Wing, *Phys. Rev. Lett.* **1980**, *45*, 631 – 634.
[110] J. van Veldhoven, H. L. Bethlem, M. Schnell, G. Meijer, *Phys. Rev. A* **2006**, *73*, 063408.
[111] F. M. H. Crompvoets, H. L. Bethlem, R. T. Jongma, G. Meijer, *Nature* **2001**, *411*, 174 – 176.
[112] F. M. H. Crompvoets, H. L. Bethlem, J. Küpper, A. J. A. van Roij, G. Meijer, *Phys. Rev. A* **2004**, *69*, 063406.
[113] C. E. Heiner, D. Carty, G. Meijer, H. L. Bethlem, *Nat. Phys.* **2007**, *3*, 115 – 118.
[114] M. R. Andrews, C. G. Townsend, H.-J. Miesner, D. S. Durfee, D. M. Kurn, W. Ketterle, *Science* **1997**, *275*, 637 – 641.
[115] C. Buggle, J. Léonard, W. von Klitzing, J. T. M. Walraven, *Phys. Rev. Lett.* **2004**, *93*, 173202.
[116] Y. V. Gott, M. S. Ioffe, V. G. Telkovsky, *Nucl. Fusion* **1962**, *3*, 1045 – 1047.
[117] D. E. Pritchard, *Phys. Rev. Lett.* **1983**, *51*, 1336 – 1339.
[118] M. Kirste, B. Sartakov, M. Schnell, G. Meijer, *Phys. Rev. A* **2009**, *79*, 051401.
[119] H. L. Bethlem, M. R. Tarbutt, J. Küpper, D. Carty, K. Wohlfart, E. A. Hinds, G. Meijer, *J. Phys. B* **2006**, *39*, R263 – R291.
[120] J. van Veldhoven, H. L. Bethlem, G. Meijer, *Phys. Rev. Lett.* **2005**, *94*, 083001.
[121] D. DeMille, D. R. Glenn, J. Petricka, *Eur. Phys. J. D* **2004**, *31*, 375 – 384.
[122] W. Paul, *Angew. Chem.* **1990**, *102*, 780 – 789; *Angew. Chem. Int. Ed. Engl.* **1990**, *29*, 739 – 748.
[123] W. Paul, *Rev. Mod. Phys.* **1990**, *62*, 531 – 540.
[124] H. L. Bethlem, J. van Veldhoven, M. Schnell, G. Meijer, *Phys. Rev. A* **2006**, *74*, 063403.
[125] M. Schnell, P. Lützow, J. van Veldhoven, H. L. Bethlem, J. Küpper, B. Friedrich, M. Schleier-Smith, H. Haak, G. Meijer, *J. Phys. Chem. A* **2007**, *111*, 7411 – 7419.
[126] P. Lützow, M. Schnell, G. Meijer, *Phys. Rev. A* **2008**, *77*, 063402.
[127] S. Schlunk, A. Marian, P. Geng, A. P. Mosk, G. Meijer, W. Schöllkopf, *Phys. Rev. Lett.* **2007**, *98*, 223002.
[128] T. Rieger, P. Windpassinger, S. A. Rangwala, G. Rempe, P. W. H. Pinkse, *Phys. Rev. Lett.* **2007**, *99*, 063001.
[129] H. L. Bethlem, M. Kajita, B. Sartakov, G. Meijer, W. Ubachs, *Eur. Phys. J. Special Topics* **2008**, *163*, 55 – 69.
[130] F. Filsinger, U. Erlekam, G. von Helden, J. Küpper, G. Meijer, *Phys. Rev. Lett.* **2008**, *100*, 133003.
[131] L. Holmegaard, J. H. Nielsen, I. Nevo, H. Stapelfeldt, F. Filsinger, J. Küpper, G. Meijer, *Phys. Rev. Lett.* **2009**, *102*, 023001.
[132] I. W. M. Smith, *Angew. Chem.* **2006**, *118*, 2908 – 2928; *Angew. Chem. Int. Ed.* **2006**, *45*, 2842 – 2861.
[133] I. R. Sims, J.-L. Queffelec, A. Defrance, C. Rebrion-Rowe, D. Travers, P. Bocherel, B. R. Rowe, I. W. M. Smith, *J. Chem. Phys.* **1994**, *100*, 4229 – 4241.
[134] N. Balakrishnan, A. Dalgarno, *Chem. Phys. Lett.* **2001**, *341*, 652 – 656. See also Erratum, ref. [162].
[135] E. P. Wigner, *Phys. Rev.* **1948**, *73*, 1002 – 1009.
[136] E. H. Taylor, Sheldon Datz, *J. Chem. Phys.* **1955**, *23*, 1711 – 1718.
[137] M. Shapiro, P. Brumer, *Principles of the Quantum Control of Molecular Processes*, Wiley, New York, **2003**.
[138] D. J. Tannor, R. Kosloff, S. A. Rice, *J. Chem. Phys.* **1986**, *85*, 5805 – 5820.
[139] R. J. Levis, G. M. Menkir, H. Rabitz, *Science* **2001**, *292*, 709 – 713.
[140] S. A. Rice, M. Zhao, *Optical Control of Molecular Dynamics*, Wiley, New York, **2000**.
[141] J. Aldegunde, J. M. Alvarino, M. P. de Miranda, V. Sáez Rábanos, F. J. Aoiz, *J. Chem. Phys.* **2006**, *125*, 133104.
[142] R. V. Krems, *Phys. Chem. Chem. Phys.* **2008**, *10*, 4079 – 4092.
[143] "Cold collisions: chemistry at ultra-low temperatures": G. C. Groenenboom, L. M. C. Janssen in *Tutorials in Molecular Reaction Dynamics* (Eds.: M. Brouard, C. Vallance), RSC, Cambridge, **2009**.
[144] A. Görlitz, A. P. Chikkatur, W. Ketterle, *Phys. Rev. A* **2001**, *63*, 041601.
[145] J. J. Gilijamse, S. Hoekstra, S. Y. T. van de Meerakker, G. C. Groenenboom, G. Meijer, *Science* **2006**, *313*, 1617 – 1620.
[146] S. Willitsch, M. T. Bell, A. D. Gingell, S. R. Procter, T. P. Softley, *Phys. Rev. Lett.* **2008**, *100*, 043203.
[147] R. Otto, J. Mikosch, S. Trippel, M. Weidemüller, R. Wester, *Phys. Rev. Lett.* **2008**, *101*, 063201.
[148] R. T. Jongma, G. Berden, G. Meijer, *J. Chem. Phys.* **1997**, *107*, 7034 – 7040.
[149] M. Drabbels, A. M. Wodtke, *J. Chem. Phys.* **1997**, *106*, 3024 – 3028.
[150] R. T. Jongma, G. Berden, T. Rasing, H. Zacharias, G. Meijer, *Chem. Phys. Lett.* **1997**, *273*, 147 – 152.
[151] M. P. J. van der Loo, G. C. Groenenboom, *J. Chem. Phys.* **2007**, *126*, 114314.
[152] L. Santos, G. V. Shlyapnikov, P. Zoller, M. Lewenstein, *Phys. Rev. Lett.* **2000**, *85*, 1791 – 1794.
[153] M. Baranov, L. Dobrek, K. Góral, L. Santos, M. Lewenstein, *Phys. Scr.* **2002**, *102*, 74 – 81.
[154] R. V. Krems, *Int. Rev. Phys. Chem.* **2005**, *24*, 99 – 118.
[155] T. Koch, T. Lahaye, J. Metz, B. Fröhlich, A. Griesmaier, T. Pfau, *Nature Phys. Sci.***2008**, *4*, 218 – 222.
[156] T. Lahaye, T. Koch, B. Fröhlich, M. Fattori, J. Metz, A. Griesmaier, S. Giovanazzi, T. Pfau, *Nature* **2007**, *448*, 672 – 675.
[157] D. DeMille, *Phys. Rev. Lett.* **2002**, *88*, 067901.
[158] A. André, D. DeMille, J. M. Doyle, M. D. Lukin, S. E. Maxwell, P. Rabl, R. J. Schoelkopf, P. Zoller, *Nat. Phys.* **2006**, *2*, 636 – 642.
[159] V. Vuletić, S. Chu, *Phys. Rev. Lett.* **2000**, *84*, 3787.
[160] P. Domokos, H. Ritsch, *J. Opt. Soc. Am. B* **2003**, *20*, 1098 – 1130.
[161] G. Morigi, P. W. H. Pinkse, M. Kowalewski, R. de Vivie-Riedle, *Phys. Rev. Lett.* **2007**, *99*, 073001.
[162] Erratum to ref. [134]: N. Balakrishnan, A. Dalgarno, *Chem. Phys. Lett.* **2001**, *351*, 159 – 160.
[163] S. Y. T. van de Meerakker, H. L. Bethlem, G. Meijer, *Nat. Phys.* **2008**, *4*, 595 – 602.
[164] B. van de Meerakker, G. Meijer, *Phys. Unserer Zeit* **2007**, *38*, 128 – 133.